Department of Economics- FEA/USP

The Health Benefits of Solar Power Generation: Evidence from Chile

NATHALY M. RIVERA

CRISTOBAL RUIZ-TAGLE

ELISHEBA SPILLER

WORKING PAPER SERIES № 2021-04

DEPARTMENT OF ECONOMICS, FEA-USP
WORKING PAPER Nº 2021-04

The Health Benefits of Solar Power Generation: Evidence from Chile

Nathaly M. Rivera (nmrivera@usp.br)

Cristobal Ruiz-Tagle. (J.C.Ruiz-Tagle@lse.ac.uk)

Elisheba Spiller (espiller@edf.org)

Abstract:

Renewable energy can yield social benefits through local air quality improvements and their subsequent effects on human health. We estimate some of these benefits using data gathered during the rapid adoption of large-scale solar power generation in Chile over the last decade. Relying on exogenous variation from incremental solar generation capacity over time, we find that solar energy displaces fossil fuel generation (primarily coal-fired generation) and curtails hospital admissions, particularly those due to lower respiratory diseases. These effects are noted mostly in cities downwind of displaced fossil fuel generation and are present across all age groups. Our results document the existence of an additional channel through which renewable energy can increase social welfare.

Keywords: Coal-fired power plants; coal displacement; solar generation; power plants; pollution; morbidity; developing countries; Latin America

JEL Codes: I18; L94; Q42; Q53

The Health Benefits of Solar Power Generation: Evidence from Chile*†

Nathaly M. Rivera‡

University of São Paulo

Cristobal Ruiz-Tagle

London School of Economics and Political Science

Elisheba Spiller

Environmental Defense Fund

This Version: February 2021

Abstract

Renewable energy can yield social benefits through local air quality improvements and their subsequent effects on human health. We estimate some of these benefits using data gathered during the rapid adoption of large-scale solar power generation in Chile over the last decade. Relying on exogenous variation from incremental solar generation capacity over time, we find that solar energy displaces fossil fuel generation (primarily coal-fired generation) and curtails hospital admissions, particularly those due to lower respiratory diseases. These effects are noted mostly in cities downwind of displaced fossil fuel generation and are present across all age groups. Our results document the existence of an additional channel through which renewable energy can increase social welfare.

Keywords: Coal-fired power plants, coal displacement, solar generation, power plants, pollution, morbidity, developing countries, Latin America
JEL classification numbers: I18, L94, Q42, Q53

*We thank Andrew Bibler, Janet Currie, Harrison Fell, Maria Harris, Nicolai Kuminoff, Subhrendu K. Pattanayak and Brett Watson for helpful comments and suggestions. We also thank seminar participants at Environmental Defense Fund, Universidad Adolfo Ibañez, Universidad Católica del Norte, University of São Paulo, and conference participants at the 21st Annual CU Environmental and Resource Economics Workshop, the Association of Environmental and Resource Economists Annual Summer Conference 2019, Camp Resources XXVI, Eastern Economic Association Annual Meeting 2020, the 25th Annual Conference of the European Association of Environmental and Resource Economists, and SETI Annual Meeting 2019, for helpful comments and suggestions. All errors are ours.

†Authors' contributions to the current version were as follows, with ∼ denoting equal contribution. Conceptualization: NR∼CR∼BS. Methodology: NR, BS, CR. Data Curation: NR, CR, BS. Empirical Analysis: NR, BS, CR. Writing Original Draft: BS, NR.

‡Corresponding author. ✉: nmrivera@usp.br.

1 Introduction

Renewable energy is the world's fastest-growing energy source, set to become the leading source of primary energy consumption by 2050 (U.S. Energy Information Administration, 2019). It promises several benefits to society, ranging from reductions in greenhouse gas emissions, lower discharge of local air pollutants and improved health outcomes, to a reduced dependence on imported fuels and the creation of jobs through the manufacturing and installation of these resources (U.S. Environmental Protection Agency, 2019). Yet, we still lack a good understanding of the magnitude of some of these benefits, notably those associated with health improvements. In this work, we use the rapid adoption of large-scale solar power generation in the desert region of northern Chile to empirically quantify some of the health benefits of solar energy.

Fossil fuel power generation, particularly that from coal combustion, releases large amounts of local air pollutants, including sulfur dioxide (SO_2), nitrogen oxides (NO_X), mercury (Hg) and particulate matter (PM). All of these pollutants are associated with several adverse health effects, along with increased hospital admissions, mortality risks and threats to life expectancy.[1] The extent to which these emissions are curtailed with the introduction of renewables reflects the potential of alternative energy sources to offset some of the negative effects of dirty electricity generation. Nonetheless, some fossil fuel plants (e.g., natural gas plants) have consistently been dispatched to deal with the intermittency of renewables (Fell and Linn, 2013), thus attenuating the benefits of increasing the supply of these sources. More insights on the co-benefits of renewable energy are, therefore, crucial to the cost–benefit analyses of transitioning away from fossil fuels and, thus, for the optimal design of energy policy.

The Atacama Desert, one of the sunniest and driest deserts in the world, not only has the highest average surface solar radiation worldwide (Rondanelli et al., 2015), but also the highest solar power potential. Figure 1 shows Chile's photovoltaic power potential—a solar energy system's maximum productivity over time—relative to the rest of the world. This potential, together with the recent decline in the cost of photovoltaic (PV) technology and the country's regulations aimed at fostering the adoption of renewables, resulted in rapid market penetration of solar generation in Chile. By the end of 2012, a variety of solar plants with capacity ranging from 3 MW to 138 MW were already injecting electricity into Chile's northern electric grid. We take advantage of this surge in large-scale investment in solar

[1] For comprehensive reviews, see Currie et al. (2014) on the effects of early-life exposure to pollution, and Hoek et al. (2013) on the mortality impact of long-term air pollution exposure.

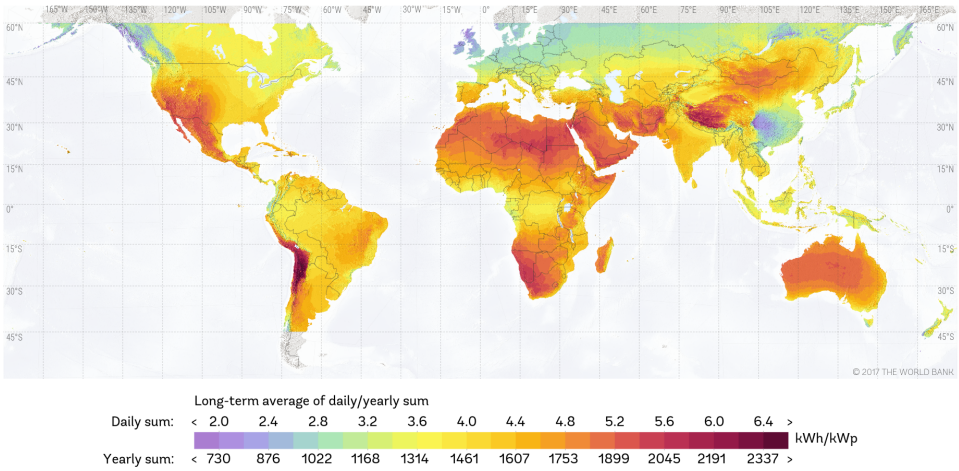

Figure 1: Chile's Photovoltaic Power Potential (kWh/kWp)

Notes: Graph retrieved from https://globalsolaratlas.info. Solar resource data obtained from the *Global Solar Atlas*, owned by the World Bank Group and provided by Solargis. Photovoltaic power potential refers to how much energy (kWh) is produced per kilowatt peak (kWp) of a system.

energy to explore the effects of the steady expansion in solar capacity on generation from thermal plants and on human health in northern Chile. By exploring the case of Chile, we add to the scant literature on power plant pollution exposure and health impacts in emerging economies (Gupta and Spears, 2017; Barrows et al., 2018).

Our study uses data on solar generation between 2012 and 2017. To identify the effects of this increasing solar expansion, we first estimate the extent to which solar plants displace other power facilities using daily variation in plant-level power generation capacity.[2] For solar generation to have a positive effect on health outcomes, it must first displace generation by thermal plants.[3] Next, we estimate a reduced form equation on the effect of daily solar generation on health. In particular, we measure health effects using data on daily hospital admissions of patients with health conditions generally associated with the combustion of fossil fuels, and we estimate a set of zero-inflated negative binomial (ZINB) regressions that relate daily solar variation to these admissions. Using limited data on fine PM concentrations, we complement this analysis with an instrumental variable control function approach that uses solar generation as an instrument for pollution in our health regressions. Throughout all of our health equations, we indirectly take into account the transport of pollutants by

[2]Ideally, we would use plant-level emissions data. Unfortunately, publicly available emissions data in Chile are engineering estimates, rather than observed or measured data.

[3]The alternative is that solar generation rises to meet expanding demands for electricity. In this case, there would be no displacement of fossil fuel plants, and the health impacts of the energy system would remain unchanged, although health improvements would have been seen relative to a counterfactual of increased fossil fuel generation in response to increased loads.

focusing on cities downwind of displaced fossil fuel plants.

Our results show that increased solar generation in Chile led to a displacement of daily thermal generation, particularly of coal- and gas-fired power generation. Subsequently, we find that, through this displacement, solar generation reduces cardiovascular and respiratory admissions in all cities included in our sample. Our analysis by age group indicates that these reductions are mostly observed among infants, children (ages 6–14) and seniors, the most vulnerable age groups. The reductions are found primarily after a short-term exposure to abated pollution from displaced thermal plants, and in cities downwind of these displaced facilities or that have fossil fuel generators within their borders. These conclusions remain unchanged after several robustness checks, which include the use of cities upwind of displaced facilities and those downwind of nondisplaced units, and the use of hospital admissions of patients with diseases presumably not related to air pollution.

Our findings can be considered a lower bound on the true health benefits from solar generation, particularly in developing countries. First, our area of study (Chile's northern region) has limited healthcare infrastructure, and thus any reduction in hospitalizations can have a beneficial spillover effect in terms of increasing the number of hospital beds available, in turn helping reduce the number of untreated unrelated injuries and illnesses. Second, reductions in air pollution exposure for young children and infants has a lifelong benefit in terms of reduced illnesses and improved economic outcomes (Currie et al., 2014). Third, the poor and minorities may live closer to large air polluters in Chile, as has been demonstrated in both the U.S. and India (e.g., Banzhaf et al. (2019); Kopas et al. (2020)). In this case, improvements in air quality may not only bring greater long-term benefits on populations experiencing uneven exposure to air pollution, but also help to reduce inequality.[4]

A wide number of papers document the displacement of coal-fired power plants, either through a decline in the price of natural gas (Lu et al., 2012; Linn et al., 2014; Knittel et al., 2015; Cullen and Mansur, 2017; Holladay and LaRiviere, 2017; Linn and Muehlenbachs, 2018), through the expansion in renewable generation capacity (Kaffine et al., 2013; Cullen, 2013; Novan, 2015; Callaway et al., 2018; Fell et al., 2019), or through interaction between the two (Holladay and LaRiviere, 2017; Fell and Kaffine, 2018). These studies also document significant interactions among competing renewables, whereby solar generation can lead to a shift in the supply of hydropower. To the extent that renewables offset and displace one another, the injection of new renewable sources into the grid may lead to am-

[4]Previous evidence shows indications of population sorting in Chile in relation to other environmental disamenities, such as mining. For example, Rivera (2020) finds that residential properties near mining sites have lower values and that these values are particularly salient for new residents in the area, suggesting an environmental-based sorting.

biguous environmental impacts. One of the benefits of conducting this analysis in northern Chile is the small amount of non-solar renewables on the grid during the study period (they made up only 6% of total capacity in 2017, combined). This allows us to isolate the effect of solar generation on fossil fuel displacement more clearly.

We extend this previous literature by empirically documenting some of the consequences of the displacement on morbidity outcomes. A small subset of literature estimates the effect of changes in the power sector on health. For example, Burney (2020) estimates the health benefits associated with the shift from coal to natural gas combustion in the U.S., finding that the exit of coal-fired plants between 2005 and 2016 saved approximately 26,000 lives. Along those lines, Casey et al. (2018a) find that coal and oil power plant retirement in the U.S. led to improvements in fertility outcomes, and Casey et al. (2018b) show the link between these retirements and a decrease in preterm births among nearby populations. Our work adds to this literature, presenting new evidence on the benefits that curtailing coal-fired generation has on morbidity. Moreover, we estimate this impact even without coal plant retirement; rather, we are able to identify the health benefits of having a large amount of solar generation at the intensive margin, even if it does not lead to coal plant shutdowns. In doing so, we contribute to quantifying the value of curtailing coal-fired generation.

The analysis of solar generation also represents an advantage in evaluating the health benefits of renewables relative to other similar sources such as wind. Increases in wind power generation may be associated with reduced pollution due to higher wind speeds and greater dispersion, hampering the identification of health impacts. There is existing work identifying the health benefits of a cleaner grid (e.g., Anenberg et al. (2012); Muller and Mendelsohn (2009)) or the addition of new utility-scale solar capacity (e.g., Sergi et al. (2020)) in integrated assessment frameworks. The latter employ cutting-edge air transport and chemical transformation models, but use existing epidemiological literature and underlying health and population statistics to calculate the impact of policies on health. To the best of our knowledge, we are the first to *empirically* test the impact of increased large-scale solar generation on health. Therefore, our work also adds to the growing literature on the co-benefits of renewable generation (e.g., Siler-Evans et al. (2013); Barbose et al. (2016); Buonocore et al. (2016); Spiller et al. (2017); Millstein et al. (2017)), a key aspect in evaluating the economic potential of renewable energy portfolios (Edenhofer et al., 2013; Wiser et al., 2017), and in the design of health-based air quality regulations (Abel et al., 2018; Thakrar et al., 2020).

The remainder of our work proceeds as follows. Section 2 reviews the literature on the health effects of power plant emissions, while Section 3 describes the power sector in Chile. Section 4 documents the data, and Section 5 presents the empirical strategy. The results

and robustness checks are in Sections 6 and 7, respectively. Section 8 concludes.

2 Power Plants' Emissions and Health Consequences

Fossil-fuel electricity generation accounts for a large share of greenhouse gas emissions, particularly carbon dioxide (CO_2), an important contributor to global warming and climate change (Stocker et al., 2013). The sector is also a major driver of outdoor air pollution, primarily due to the burning of coal, which releases an important amount of airborne pollutants such as SO_2, NO_X, Hg and PM. All of these pollutants are associated with adverse health effects, mortality risks and threats to life expectancy (e.g., Chay and Greenstone (2003a,b); Currie and Neidell (2005); Bateson and Schwartz (2007); Currie et al. (2009); Chen et al. (2013); Arceo et al. (2016); Knittel et al. (2016); Schlenker and Walker (2016)). Coal combustion also affects water quality. Ash released after coal combustion can end up in water reservoirs, contaminating waterways and sources of drinking water (Carlson and Adriano, 1993). Here, we briefly summarize the evidence on the detrimental health impact of exposure to the main pollutants from coal combustion. Evidence suggests that its displacement by solar generation is expected to curtail mostly SO_2, PM and NO_X emissions.

SO_2 is an invisible gas, part of the sulfur oxide (SO_X) family of gases, formed when fuel containing sulfur (e.g., coal, oil) is burned during metal smelting or other industrial processes (U.S. Environmental Protection Agency, 2014). Exposure to high concentrations of this pollutant is associated with eye, nose, and throat irritation, infectious complications of chronic obstructive pulmonary disease, and rises in hospital admissions due to obstructions of the lower airway such as asthma (World Health Organization, 2006). SO_2 reacts with other compounds in the atmosphere to form fine PM. Particulate matter is the general term used to describe solid particles, dust and drops found in the air, all with different compositions and sizes. Evidence on the health impact of exposure to coarse PM (PM_{10}) and fine PM ($PM_{2.5}$) suggests detrimental effects on a variety of health outcomes, including respiratory diseases (Schwartz, 1996; Coneus and Spiess, 2010), cardiovascular diseases (Schwartz and Morris, 1995; Brook et al., 2010; Franklin et al., 2015), low birth weight (Currie et al., 2009; Coneus and Spiess, 2010; Currie and Walker, 2011), and infant mortality (Chay and Greenstone, 2003a,b; Arceo et al., 2016; Knittel et al., 2016).

NO_X are reactive gases, and include nitrogen dioxide (NO_2), nitrous acid (HNO_2) and nitric acid (HNO_3). Although mobile sources are responsible for the highest domestic anthropogenic release of NO_X into the atmosphere, stationary fossil fuel combustion represents a

significant portion of annual domestic NO_X emissions. Evidence on outdoor exposure to NO_X indicates rises in asthma and bronchitis diagnoses in children (Orehek et al. (1976); Pershagen et al. (1995); Chauhan et al. (2003); Gauderman et al. (2005)), and older populations (Schlenker and Walker, 2016). This pollutant can also react in the presence of heat and sunlight in the atmosphere to create ground-level ozone, a harmful chemical associated with lung diseases and premature deaths (Bell et al., 2004, 2005).

Hg is a toxic pollutant present in rocks, including coal in its natural state. Burning coal releases Hg into the air, and it eventually settles into waterbodies through atmospheric deposition. Once in the water, Hg is transformed by aquatic microbes into methylmercury ($[CH_3Hg]^+$), a poisonous form of mercury that accumulates in fish. Eating contaminated fish is associated with cardiovascular diseases (Salonen et al., 1995; Guallar et al., 2002), and with damage to the central nervous system in unborn (Clarkson, 1990). In the same way, high blood Hg levels have been associated with elevated risk of IQ loss among children (Trasande et al., 2005). Currently, coal-fired power plants represent the largest source of domestic anthropogenic emissions of this global air pollutant (U.S. Environmental Protection Agency, 2015).

Evidence on the health impact of exposure to power plant pollution is limited within the Chilean context. Epidemiological research from Ruiz-Rudolph et al. (2016) show significantly higher rates of cardiovascular and respiratory hospital admissions in Chilean municipalities that host power plants and other large-scale polluters. Yet, the authors fail to take into account proximity to the pollution source, or the air transport of pollutants in the vicinity of these facilities. This further highlights the importance of our work—identifying a causal impact of exposure to power plant pollution on respiratory and cardiovascular hospitalizations in Chile by relying on an exogenous source of variation: the incremental solar electricity generation capacity over time.

3 The Power Sector in Chile

The electricity sector in Chile is composed of three different segments: generation, transmission and distribution, all 100% privately owned. The sector is dominated by fossil fuels, which account for 53% of total generation, followed by hydro with 28%. The fossil fuel generation mix is primarily coal (40%), followed closely by natural gas (36%) and petroleum (24%) (Comisión Nacional de Energía, 2018).

Before 2018, Chile's electricity market featured four different electric systems (see Figure

2): two major interconnected systems, the Northern Interconnected System (Sistema Interconectado del Norte Grande — SING) and the Central Interconnected System (Sistema Interconectado Central — SIC); and two additional minor grids, the Aysen Electric System (Sistema Eléctrico de Aysen — SEA) and the Magallanes Electric System (Sistema Eléctrico de Magallanges — SEM). The SING system, located in Chile's northern region, has 5 GW of installed capacity, 2.5 GW of peak load and more than 85% reliance on fossil fuel generation (i.e., coal, natural gas and diesel). Although the northern region of Chile is relatively unpopulated, with SING serving only 7% of the country's total population, this region hosts most of the large-scale copper mining companies that operate in the country, a sector characterized by its electricity-intensive production activities.[5] Conversely, the SIC system, located in central-south Chile and with 17 GW of total installed capacity and 7 GW of peak load, relies heavily on hydro generation (around 35%) and serves 90% of the country's population. These two major grids, SING and SIC, began an interconnection process in November 2017 that resulted in a full integration by May 2019, thereby creating Chile's National Electric System (Sistema Eléctrico Nacional — SEN). In this paper, we focus on the period before November 2017, thus avoiding any potentially confounding factors that may be associated with the interconnection itself.

3.1 The Generation Segment

Chile's current electric service legislation offers established competitive conditions in the generation segment and maintains regulatory conditions for the transmission and distribution segments. Generation at SING is characterized by a spot market, long-term forward contracts and capacity payments. The spot market is a merit-order dispatch model that operates under the coordination of the Economic Load Dispatch Center (Centro de Despacho Económico de Carga — CDEC), which dispatches generators based strictly on their marginal cost at every hour to meet the system's load. The marginal cost of the system is set at every hour by the CDEC and equals the cost of the most expensive unit being dispatched (Galetovic and Muñoz, 2011).[6] This dispatch, determined by the regulator based on fuel costs, informs our methodology in estimating the displacement of fossil fuel plants by solar generation. Specifically, we incorporate relative costs of fossil fuels into our dispatch equation to control for the market forces that will play a large role in determining dispatch and the ability of

[5] During 2016, the copper industry consumed 50,578 TJ of electricity supplied by SING. This consumption was equivalent to more than 30% of SING's installed capacity of 5 GW (data retrieved in May 2020 from https://www.cochilco.cl).

[6] Regardless of whether generators are dispatched or not, each of these agents receives a monthly capacity payment aimed at guaranteeing enough generation capacity to supply energy during times of peak demand.

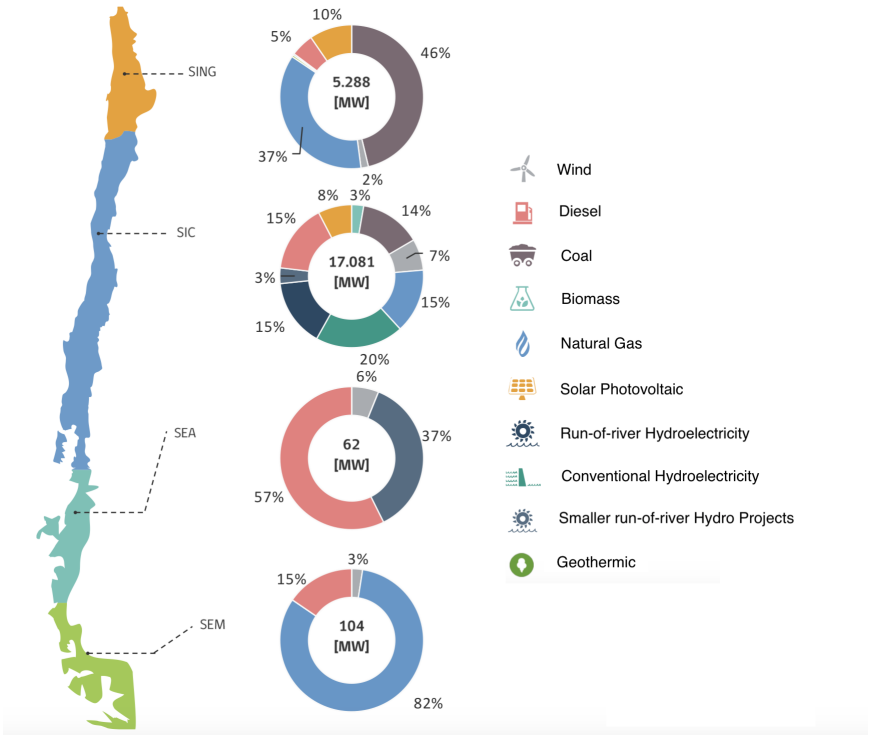

Figure 2: Bulk Power Systems in Chile

Notes: Adapted from the *National Energy Commission Monthly Report*, December 2017. https://www.cne.cl/wp-content/uploads/2015/06/RMensual_v201712.pdf

solar to displace fossil fuel plants (see Section 5.1).

3.1.1 Solar Generation

Although numerous PV systems have existed in Chile since 2007, they were originally mostly in the form of small-scale stand-alone systems and formed part of rural electrification programs (Haas et al., 2018). In 2008, however, the Chilean government established a quota system for renewable energies; this currently requires that these sources account for 20% of participation in the energy mix by 2025 (Ministry of Energy, 2013). This policy, in combination with decreasing costs in PV technology, led to the installation in 2012 of the first large-scale solar plant in northern Chile, La Huayca, adding 25.05 MW of gross capacity to SING. By 2015, solar participation at SING reached 119 MW, equivalent to 2% of the total daily generation of the system (≈.376 GWh), and by the end of 2017 it had grown to 655 MW, equivalent to 10% (≈1.5 GWh).[7]

[7]Data retrieved from the annual reports of Chile's National Energy Commission (Comisión Nacional de Energía — CNE), https://www.cne.cl/nuestros-servicios/reportes/informacion-y-estadisticas/

3.1.2 Emissions

Due to Chile's heavy reliance on fossil fuels, the power sector accounts for approximately 40% of the nation's total greenhouse gas emissions, which translates as 34,568.2 kt and 1.6 kt of carbon dioxide equivalent emissions (CO_2e) due to CO_2 and methane (CH_4) discharges, respectively (Chile Environmental Ministry, 2018). In terms of criteria air pollutants, the sector accounts for more than 30% of the country's total NO_X and SO_2 emissions, two hazardous pollutants common to coal combustion (see Section 2). This situation is aggravated by the longevity of some fossil fuel power plants, as older plants generally emit more. At SING, for instance, some coal-fired generators are the oldest in the country, with ages that in some cases exceed 50 years (Programa Chile Sustentable, 2017). Annual discharges from the sector in this region are equivalent to 57% and 40% of Chile's total SO_2 and NO_X emissions, respectively (Chile Environmental Ministry, 2017), with concentration readings that generally exceed life-threatening levels.

As an example, Figure 3 plots the hourly average SO_2 (a) and NO_X (b) concentrations in Tocopilla, the city with the highest number of coal-fired power plants in SING, before (solid line) and after (dashed line) the first solar connection, in 2012. As observed in both panels, there is a clear decrease in hourly average concentrations of these two pollutants after the introduction of large-scale solar installations in the system, although NO_X levels decrease much more drastically than SO_2. To the extent that these reductions are effectively due to the entry of new solar installations, Figure 3 anticipates the potential health benefits of a cleaner grid. In any case, SO_2 and NO_X hourly averages in this city still exceed U.S. EPA standards, currently set at 200 $\mu g/m^3$ for 1-hour SO_2 concentrations, and 100 ppb for NO_2, the most prevalent form of NO_X in the atmosphere.

Regarding PM, Chile has relatively high daily average $PM_{2.5}$ concentrations. For instance, national annual average concentrations reached 21 $\mu g/m^3$ in 2017, well above the World Health Organization (WHO) guidelines (10 $\mu g/m^3$ per year), which in the country's north is largely due to the region's dependence on fossil fuel power generation (Chile Environmental Ministry, 2017).[8] Figure 4 shows daily average $PM_{2.5}$ concentrations in Tocopilla between 2009 and 2019. As shown, concentrations have decreased over time but still exceed WHO standards for 24-hour averages (25 $\mu g/m^3$) during certain times of the year. This highlights the importance that solar-powered electricity can play in reducing environmental-related health concerns in areas with a heavy reliance on fossil fuels.

[8]The power sector is also the largest emitter of direct discharges of pollutants into the ocean and coastal waters in Chile's northern region (Chile Environmental Ministry, 2017).

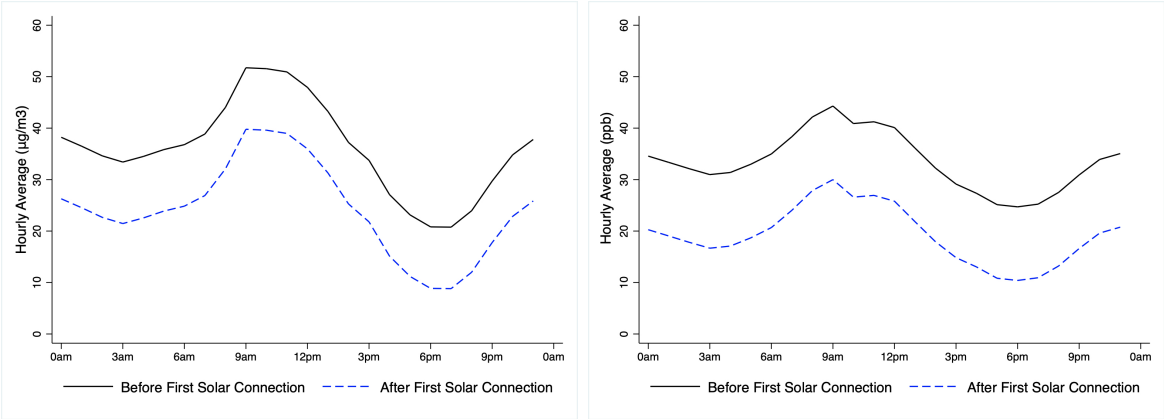

(a) SO_2 (b) NO_X

Figure 3: Hourly Sulfur Dioxide (SO_2) and Nitrogen Oxide (NO_X) Concentrations in Tocopilla

Notes: Hourly averages are obtained after controlling for a quadratic time trend. "Before the first solar connection" includes observations between 2007 and 2011. "After the first solar connection" includes data between 2013 and 2017. SO_2 is measured in micrograms per cubic meter of air ($\mu g/m^3$), and NO_X in parts per billion (ppb).

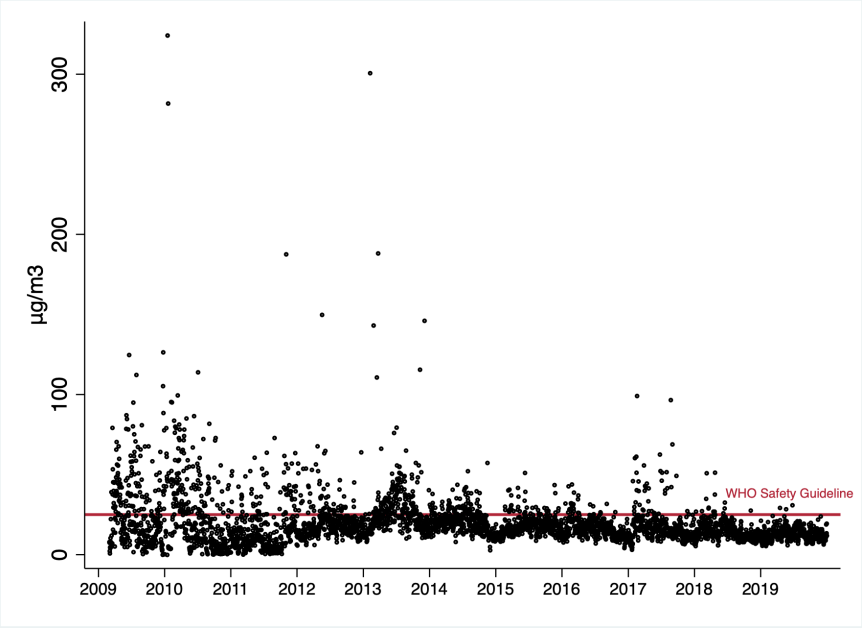

Figure 4: Tocopilla's Daily Average $PM_{2.5}$ Concentrations

Notes: Reference line represents the World Health Organization's 24-hour mean guideline of 25 $\mu g/m^3$. Data from Tocopilla's stations at the National Air Quality Information System (Sistema de Información Nacional de Calidad del Aire — SINCA), https://sinca.mma.gob.cl

Preferably, the main hypothesis of this paper would be tested using data similar to those in Figures 3 and 4. Unfortunately, however, we lack comprehensive city-level data on airborne

pollution for all the cities in our sample, as air quality monitoring stations in Chile are scarce for cities other than Santiago. We address this limitation with our displacement analysis. Later in the paper, we do use the only available data on $PM_{2.5}$ concentrations for some of the cities in our sample as an additional test on our results (see Section 6.2.2).

4 Data

4.1 Plant-Level Data

We obtain comprehensive plant-level data on daily power generation from the National Electricity Coordinator (Coordinador Eléctrico Nacional — CEN), the national body in charge of SING. Along with the information on generation, the data include specifics on plant-level technology and capacity, which we later merge with data on fuel use and prices obtained from the National Energy Commission (Comisión Nacional de Energía — CNE). As November 2017 was the month in which SING and SIC were first connected, our sample covers the years 2012 to 2017. Descriptive statistics for daily generation are presented in Table 1 by energy source, while fuel use and prices are presented in panels A and B, respectively, of Table 2.

Table 1: Daily SING Generation (GWh) by Plant Primary Fuel Source

Energy Source	Obs.	Mean	Std. Dev.	Min.	Max.	Initial Year: 2012		Final Year: 2017	
						#EGUs	Cap. (MW)	#EGUs	Cap. (MW)
Coal	2,192	39.36	3.68	17.62	49.04	13	1,959	15	2,449
Diesel	2,192	.12	.19	0	1.99	12	117	13	117
Fuel oil	1,187	0.07	0.12	0	0.63	3	36	3	36
Fuel oil #6	2,192	0.37	0.49	0	2.30	4	177	7	50
Natural gas	2,192	5.03	2.18	0	17.29	5	1,368	6	1,925
Hydro	2,192	0.21	0.03	0.07	0.33	4	16	5	17
Geothermal	306	0.21	0.20	0	0.73	-	-	2	79
Wind	1,492	.84	.47	0	2.78	-	-	2	200
Solar	1,918	1.46	1.60	0	6.09	1	25	18	655

Notes: Observations are plant-days. EGUs are electric generating units. Capacity (cap.) is the average net capacity for the given year. All gas-fired power plants are combined-cycle (CC) plants that also run with diesel.

Table 1 shows that coal-fired electric generating units (EGUs) are SING's main source of power generation, with an average of 39.36 GWh per day, followed by gas-fired units with 5.03 GWh, and solar units with 1.46 GWh. This is consistent with the amount of fuel

Table 2: Monthly Fuel Use and Prices

Variable	Mean	Std. Dev.	Min.	Max.	Obs.
Panel A. Fuel Use					
Coal	34,931.76	3,210.30	25,949.25	42,148.77	2,192
Diesel	1,020.77	684.61	26.08	2,602.4	2,192
Fuel oil	369.33	301.059	1	1,219	1,187
Fuel oil #6	955.93	910.55	9	3,321.5	2,192
Natural gas	15,333.87	7,389.24	3,371.79	44,707.66	2,192
Panel B. Fuel Prices					
Coal	105.41	16.21	68.19	138.73	2,192
Diesel	620.94	200.63	288.5	908.7	2,192
Fuel oil	95.79	22.91	46.67	125.33	1,187
Fuel oil #6	446.96	175.40	157	728.41	2,192
Natural gas	3.15	0.79	1.7	5.94	2,192

Notes: Using main fuel source only. Coal, diesel and fuel oil are in tons, while natural gas is in thousands m^3. Prices are in US$/ton for coal, US$/m^3 for diesel and fuel oil #6, in US$/mm btu for natural gas, and in US$/bbl for fuel oil.

used by these sources, as coal and gas plants report the greatest usage in Table 2. From Table 1, we also observe that coal-fired and hydroelectric plants are always dispatching in our sample, as revealed by the positive minimum daily generation. Furthermore, solar generation experienced the highest growth in terms of the number of new units and capacity installed into the system, as shown in the last four columns of Table 1.[9]

Figure 5 depicts the share of SING's monthly power generation by both fossil fuel and solar facilities during the sample period. At the start of the period, power generation at SING was (almost fully) coming from fossil fuels, with coal alone representing around 85% and natural gas roughly covering the other 15%. Although there was some solar generation by the end of 2012, a significant injection of solar-generated energy started at the beginning of 2015. As shown in the same figure, this injection coincides with the persistent decrease in fossil fuel power generation over the same period. By the end of 2017, coal-generated electricity represented around 77% of SING's monthly generation, while natural gas use was equivalent to less than 10%.[10]

[9]Note in Table 1 that the total net capacity of plants running with fuel oil #6 decreased from 177 MW in 2012 to 50 MW in 2017. This is due to the closure of two main generators, units U10 and U11, part of Termoelectrica Tocopilla, a power plant in operation since 1960. In fact, four generators were closed during the sample period. Although solar generation may also displace fossil fuel generation at the extensive margin, our main analysis is conservative as it is centered around the effects of displacement at the intensive margin only. If these shutdowns were a consequence of the injection of solar power into the system, our estimates would thus constitute a lower bound of the true effect of solar power generation on improved health outcomes.

[10]Figure A1 in the Appendix shows SING's daily load over the sample period. The increasing trend in demand over time indicated in this graph rules out a demand-driven reduction in fossil fuel power generation.

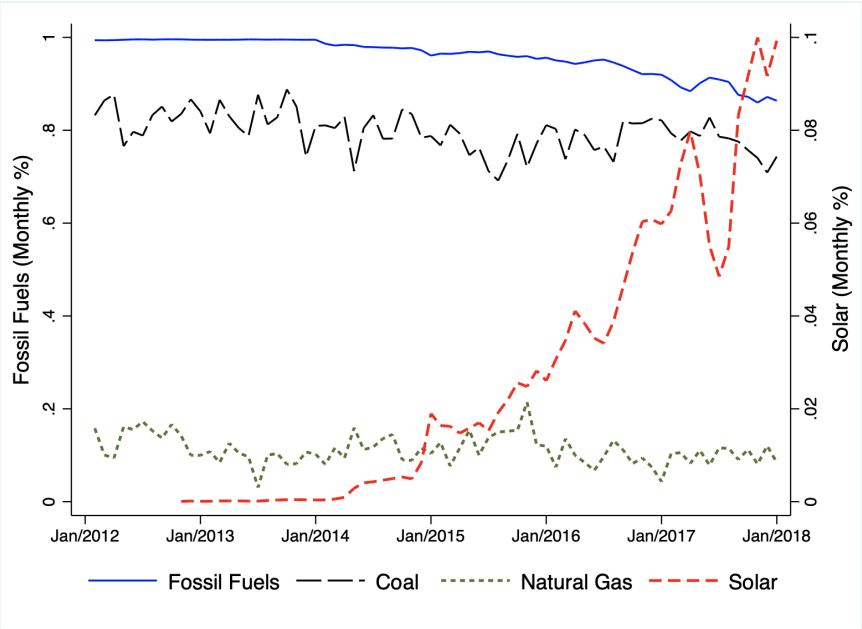

Figure 5: SING's Monthly Fossil Fuel and Solar Power Generation

A more detailed overview of the relationship between solar and other fuels is offered by Figure 6, which depicts SING's hourly generation by fuel source averaged over the first week of January 2016 (left-hand side), and the last week of October 2017 (right-hand side), just before the SING–SIC interconnection. Starting in 2016, SING had nine solar plants with 332 MW of total net capacity actively injecting power to the grid. By October 2017, this capacity had doubled to 18 active solar projects, with a total net capacity of 654 MW. When comparing these two periods in Figure 6, we observe that this increased solar capacity largely displaced hourly coal- and gas-fired combustion during Atacama's sunlight hours (7 a.m.–7 p.m.).

4.2 Health Outcomes

We use data from the Department of Health Statistics and Information (Departamento de Estadísticas e Información de Salud — DEIS), part of Chile's Ministry of Public Health, from 2012 to 2017. DEIS provides data on each patient that has been discharged from any hospital, together with information on their date of admission and the physician's diagnosis of the leading cause of disease. Although the data are compiled at the hospital or urgent care center level, they include a variable on each patient's city of origin, allowing us to match the location of health outcomes with the location of generators. In our baseline specifications on health, we look at daily hospital admissions at the city level as our main outcome. We focus

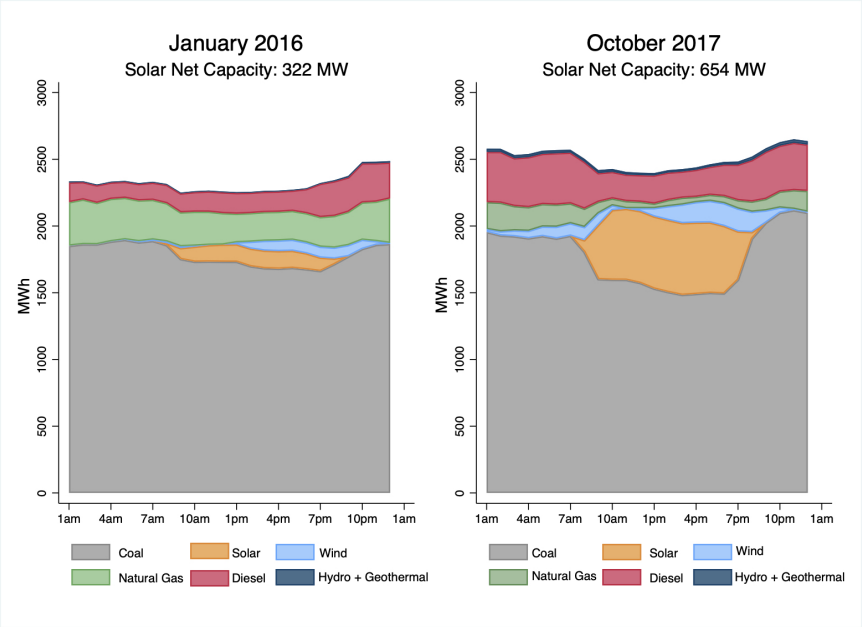

Figure 6: SING's Hourly Generation by Fuel

Notes: Total hourly generation by fuel averaged over the first week of January 2016 (left-hand side), and the last week of October 2017 (right-hand side). The left-hand side panel covers a period before the installation of nine additional solar projects, which subsequently doubled SING's total solar installed capacity. By the end of 2017, just before the SING–SIC interconnection, SING's total solar capacity had reached 654 MW (right-hand side).

on hospital admissions due to cardiovascular and respiratory conditions, and, within respiratory conditions, we further examine upper and lower respiratory infections.[11] Descriptive statistics on hospital admissions by condition are presented in Table 3 for the 19 cities in the sample.

Table 3: Descriptives on Daily Hospital Admissions

Disease	Mean	Std. Dev.	Min.	Max.	Obs.
Cardiovascular	1.028	2.162	0	36	41,648
All respiratory	1.070	2.346	0	25	41,648
Upper respiratory	0.331	1.092	0	16	41,648
Lower respiratory	0.608	1.366	0	18	41,648

Notes: Observations are at the city level.

[11] Upper respiratory infections affect the nose and throat, causing symptoms such as sneezing and coughing. Among the most frequent upper respiratory infections are the common cold, sinusitis (sinus inflammation), epiglottitis (trachea inflammation) and laryngitis (infection of the voice box). Lower respiratory infections affect the lungs and lower airways. Common lower respiratory infections are bronchitis (bronchial tube inflammation), bronchiolitis (an infection of the small airways, affecting children), pneumonia (a lung infection), asthma (long-term disease of the lungs), influenza and tuberculosis (bacterial lung infection).

4.3 Wind Direction

Our data on wind direction come from Chile's Meteorological Service and Air Quality System, and cover four cities that host fossil fuel power plants, namely Arica, Iquique, Tocopilla and Antofagasta. Mejillones also has a fossil fuel power plant but no available wind data; instead, we rely on information from the nearest available city, Antofagasta, 62 km away. The eight-wind compass roses for these cities are displayed in Figure 7 for daytime (dashed line) and nighttime (solid line) wind patterns.[12]

Although wind speed is generally higher at night, we use daytime information given our focus on the daily thermal displacement by solar energy sources. Considering that solar installations produce at peak capacity around midday, we expect daytime wind direction patterns to be more informative on a population's true exposure to reduced emissions from the displacement of fossil fuel generation during solar availability. Therefore, we obtain average wind direction by drawing a pie slice with an angle of $\pi/4$ radians (i.e. 45 degrees) bisected by average daytime wind direction in each location.[13]

4.4 Other Covariates

We also obtain information on other factors potentially correlated to hospital admissions. First, we obtain data on city-level demographic characteristics such as population, density, poverty and fertility rates as a proxy for socioeconomic factors known to affect health outcomes.[14] We gather this information from the National System of Municipalities Information (Sistema Nacional de Información Municipal — SINIM). The demographic data are updated every two years, and therefore we are able to include these variables in our estimation regressions jointly with city-fixed effects.

Data on weather come from two different sources. First, we gather information on maximum and minimum temperatures from the National System on Water Information (Sistema Nacional de Información del Agua — SNIA) for several monitoring stations located in remote areas in northern Chile. Although we obtain this information for almost all cities in our dataset, there are some incomplete entries, which we replace with daily regional averages.

[12]For the city of Iquique, we only have nighttime wind direction (see Figure 7(b)). In the definition of downwind cities, we approximate daytime wind patterns for this city using nighttime information.

[13]The resulting average wind direction is: 1.15π radians (206.9 degrees) in Arica (Figure 7(a)), 1.57π radians (282.7 degrees) in Iquique (Figure 7(b)), 1.33π radians (238.6 degrees) in Tocopilla (Figure 7(c)) and 1.09π radians (196 degrees) in Antofagasta (Figure 7(d)).

[14]Unfortunately, city-level data on other indicators such as unemployment and income are not publicly available.

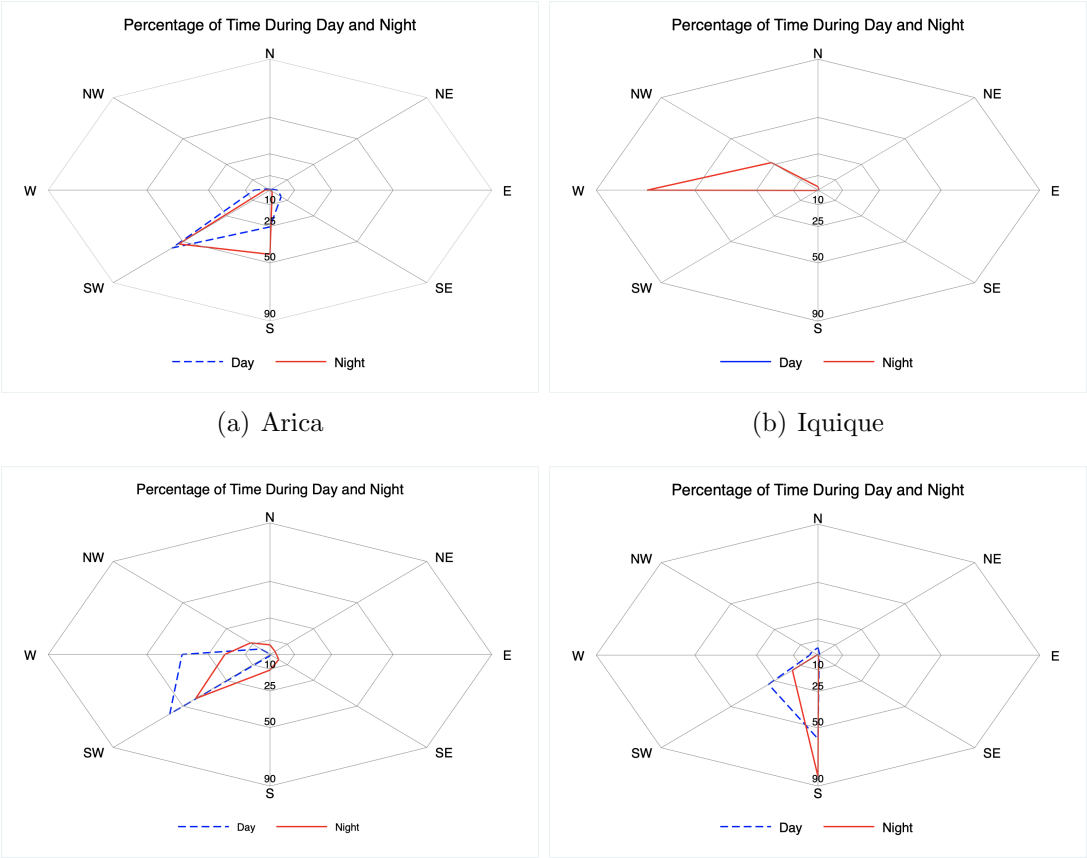

(a) Arica

(b) Iquique

(c) Tocopilla

(d) Antofagasta

Figure 7: Daily Wind Direction in Cities with Fossil Fuel Generation

Notes: "Daytime" encompasses average wind direction patterns during sunshine hours (7 a.m.–7 p.m.). "Night" encompasses average wind direction between 7 p.m. and 7 a.m. the following day. Concentric circles represent the percentage of time in which the wind blows in that direction, namely 10%, 25%, 50% and 90%. Data on daytime wind direction for Iquique (7(b)) are not available.

The second source is Solar Explorer, an initiative of the Chilean Ministry of Energy (Ministerio de Energía) that contains data on humidity for all the cities in our sample. Descriptive statistics for these covariates are in panel A of Table A1 in the Appendix.

5 Methods

5.1 Displacement

We begin by estimating the effect of solar adoption on the power generation of existing power plants from 2012 to 2017.[15] To that end, we categorize all the plants in the system by their primary fuel type (e.g., coal, diesel, natural gas, fuel oil) and then define a set of linear models of daily generation to observe which types of plant decrease or increase their production with the introduction of solar generation. Given our interest in the overall effect of solar power generation on health, we use daily-level variation as our main specification because total daily generation (and thus emissions) is more directly related to health outcomes than hourly shifts. In particular, we define aggregated generation displacement equations as follows:

$$G_d^f = \gamma_0 + \gamma_1 S_d + \sum_{j \neq f} \delta^j \left(FuelUse_m^f * \frac{P_m^f}{P_m^j} \right) + \gamma_2 Load_d + \omega_d + \tau + \epsilon_d^f, \tag{1}$$

where G_d^f is the system's generation by fuel f during day d, ω_d is a vector of daily weather covariates, τ is a vector of time-fixed effects, and ϵ_d^f is an error term. We consider two variations of τ. The first of these, τ_1, considers year, month, and weekend fixed effects, while a stronger version, τ_2, includes year, seasons, year $\times$ seasons, and weekend fixed effects.

Equation (1) also includes the variable $Load_d$ that represents the system load during day d to control for increases in demand over time, as demonstrated by Figure A1 in the Appendix.[16] In addition, Equation (1) considers a term that models SING's dispatch of generators to control for differences in input prices that may affect daily dispatch conditions. This term is given by the interaction between aggregate use of fuel f during month m, $FuelUse_m^f$, and the relative international (exogenous) monthly prices of the fuels in the system, P_m^f / P_m^j, where $f \neq j$. Importantly, we do not include relative prices with respect to solar energy or other renewables, given their zero marginal cost.

The key variable in Equation (1) is S_d, which represents the system's solar generation during day d. Whether solar power generation induces a significant displacement of non-solar sources should be reflected by the displacement parameter γ_1. We estimate Equation (1) with an ordinary least square (OLS) estimator, bootstrapping the standard errors to account for

[15] Our displacement analysis is a short- to medium-term analysis as it takes SING's infrastructure as given during our sample period (Baker et al., 2013).

[16] As the large-scale copper mining industry is an important actor in the demand for energy at SING, variations in daily load should also capture similar variations in copper production.

any heterogeneity and serial correlation in the generation data. To take into account the heterogeneous capacity across fuel types, we also estimate an alternative specification of Equation (1) in which we replace G_d^f by capacity factor CF_d^f, defined as total daily generation by fuel f weighted by its net capacity. Given that CF_d^f takes values between 0 and 1, we estimate this version of Equation (1) using a generalized least-squares (GLM) estimator assuming a logit distribution.

In addition to the aggregated generation displacement, we run a plant-level version of Equation (1) to identify the set of plants displaced by solar generation and those that are not. In this case, we modify Equation (1) to include generation G_{id}^f at the plant-level i, and their corresponding fuel use $FuelUse_{im}^f$, as follows:

$$G_{id}^f = \beta_0 + \beta_1 S_d + \sum_{j \neq f} \delta^j \left(FuelUse_{im}^f * \frac{P_m^f}{P_m^j} \right) + \beta_2 Load_d + \omega_d + \tau + \epsilon_{id}^f. \tag{2}$$

5.2 Solar Generation and Health

Once we have confirmed that fossil fuel plants are indeed displaced by daily solar generation, our next step is to estimate the resulting effect of solar power generation on health outcomes (e.g., hospital admissions) for all cities in our sample, and for cities in close proximity to these plants. A more in-depth discussion on this approach is offered in Section 5.2.1. We define our baseline health equation as follows:

$$Health_{jd} = \delta_0 + \delta_1 S_d + \omega_{jd} + \zeta + \tau + \nu_{jd}, \tag{3}$$

where $Health_{jd}$ represents a health outcome in city j during day d; ω_{jd} is a vector of daily city-level weather covariates that may affect morbidity outcomes such as daily maximum and minimum temperatures and humidity; ζ is a vector of demographics and city-fixed effects; τ is a vector of time-fixed effects; and ν_{jd} is an idiosyncratic effect. As in Equation (1), we consider two variations that include several combinations of weekend, month, season, and year fixed effects.

The main variable in Equation (3) is S_d, which measures SING's total solar generation on day d. As we construct this variable considering all solar plants in the system, daily variation in S_d is exogenous to any daily variation in hospital admissions in a given city j. Our parameter of interest in Equation (3), δ_1, gives us the marginal effect of solar generation on the health outcome of interest. We estimate Equation (3) using a ZINB model due to

the large number of zeros in the outcomes (count variables) and a clear overdispersion of these outcomes across cities in our sample.[17] While we control for population in all of our regressions, we also estimate Equation (3) with an OLS estimator on the rate of hospital admissions per 100,000 people as a robustness check.[18]

There are some potential drawbacks in the estimation of Equation (3). First, fossil fuel plants are not randomly placed across the region, so cities with and without fossil fuel plants may be observably different. Indeed, this is the case exhibited in panels B and C of Table A1 (Appendix), which shows that cities without fossil fuel plants (panel C) are smaller, less dense and poorer than those with fossil fuel plants (panel B) (all of these differences are statistically significant). Thus, in addition to city-fixed effects, we also control for demographic characteristics (e.g., poverty rate, density, fertility rate) in the estimation of Equation (3). Second, the large copper mining industry is an important actor in the demand on the energy sector in northern Chile, and also a significant air pollution emitter. For this reason, we estimate an alternative specification to Equation (3) in which we control for monthly large-scale copper production by city.[19]

Third, there may be important dynamic effects of daily avoided fossil-fueled pollution on health outcomes. As air pollution gathers and accumulates in the atmosphere over time, we would expect to see a lagged effect of daily improvements in air quality on health.[20] In particular, air quality improvements over three or four days may very well lead to greater health benefits today than contemporaneous improvements in air quality. In that case, Equation (3) would give us an incomplete picture of the actual health effect of a cleaner grid.

There is precedent in the literature for testing the effect of lagged exposure to air pollution on health. For instance, Neidell (2009) includes up to six days of lags, although the preferred specification includes only four days, while Schlenker and Walker (2016) opt for three days of lags. Although these two papers are looking at increases in air pollution, whereas our

[17] See Figure A2 (Appendix) for an example of two cities, Antofagasta and Tocopilla.

[18] It is important to note here that some cities in northern Chile are very small in size, which means that many of them report zero daily hospital admissions, particularly when it comes to admissions by age group. This complicates an OLS estimation on the rate of admissions, as in this case our outcome variable is continuous but with an important pileup at zero. Alternative estimation methods to deal with this, such as a Hurdle estimation, resulted in the lack of convergence in many of our regressions.

[19] We obtain this information from the Chilean Copper Corporation (Corporación Chilena del Cobre — COCHILCO). We would much rather use data on daily variation in production, but this information is unavailable.

[20] Indeed, there is evidence that certain air pollutants can have an extended effect on health. For instance, the U.S. Environmental Protection Agency (2006) found that ozone can have an effect on health for up to four days after exposure.

method identifies the impact of air quality improvements, we could potentially identify a dynamic effect through the inclusion of a couple of lags in our health equation. However, this is not straightforward in our setting due to the fact that our main variable of interest (solar generation) is highly colinear across days.[21] Thus, including lags and leads would result in unstable estimates due to the multicollinearity of the variables. Instead, we explore a slightly different approach by testing whether there is a cumulative impact of longer-term solar generation (and thus, longer periods of exposure to reduced fossil fuel-related pollution) on health. We do this by estimating the impact of average weekly, monthly, and yearly solar generation on health outcomes, as depicted by Equation (4) where $T = \{7, 30, 365\}$. Expressed in this way, δ_t approximates the average long-term effect of solar generation on daily hospital admissions.

$$Health_{jd} = \delta_0 + \delta_t T^{-1} \sum_{t=1}^{T} S_{d-t} + \omega_{jd} + \zeta + \tau + \nu_{jd}, \tag{4}$$

5.2.1 Air Pollution Exposure and Wind Direction

A final concern regarding Equation (3) is that it ignores the potential air transport of pollutants and, therefore, likely underestimates the effect on cities that are located closer to fossil fuel plants and more exposed to their pollution, or displacement thereof. We address this by rerunning our health equation using only those cities downwind of fossil fuel plants to (indirectly) account for the transport of pollutants.[22] To that end, we use the information from the eight-wind compass roses in Figure 7, to guide us on exposure to pollution from fossil-fueled generators.

For example, Tocopilla illustrates the case of a downwind city. From Figure 8, we can observe that it hosts two power plants in its surrounding area, both at a distance of roughly 2 km and southwest from the city center.[23] Combining this information with the prevailing wind at this location (see Figure 7(c)), we observe that daytime wind blows from the southwest more than 50% of the time, and from the west 40% of the time.[24] Considering the location of the thermal plants in Figure 8, it is straightforward to conclude that Tocopilla is downwind of their emissions. Using similar information for all the cities that host thermal plants, we can

[21] Our multicollinearity tests between $Solar_d$ and $Solar_{d-l}$ for $l = \{1, 2, 3\}$ reveal variance inflation factors (VIFs) of magnitudes close to a 100.

[22] We state "indirectly" here because we do not have emissions data; thus, being downwind of a displaced plant only creates a proxy for potential to be in the line of emissions.

[23] More specifically, at an angle of 217 degrees from the city's geographical centroid.

[24] Any other wind direction amounts to less than 5% during daytime.

Figure 8: Power Plant Locations in Tocopilla

Notes: Map of Tocopilla with the location of two fossil fuel power plants and the likely downwind area given the prevailing daytime wind direction.

identify those that are downwind of thermal power generation. Furthermore, we combine this information with the displacement results to construct an indicator for whether a city is downwind of a displaced plant. In particular, we use four different categories throughout the description of our health results: all cities, and cities downwind of displaced fossil fuel plants that are located within $10km$, within $50km$ or within $100km$ of their boundaries. In addition, we can identify cities downwind of nondisplaced fossil fuel plants and those upwind of displaced fossil fuel plants to use later in our robustness analyses.

6 Results

6.1 Fossil Fuel Displacement

Tables 4 and 5 present the results of the effect of 1-GWh of daily solar generation on the displacement of daily aggregated generation (Equation (1)) for fossil fuels and renewable sources, respectively. From left to right, each column shows a specification with more controls. The two tables also include the effect of 1-GWh of daily solar generation on capacity factors.

Our findings in Tables 4 and 5 suggest that solar-generated electricity displaces other fuel sources, particularly dirty sources. From Table 4, we observe that a 1-GWh increase in daily

Table 4: The Effect of 1 GWh of Solar Power Generation on Daily Aggregated Fossil Fuel Power Generation

	Coal		Diesel		Fuel oil		Fuel oil #6		Natural gas	
	(1)	(2)	(1)	(2)	(1)	(2)	(1)	(2)	(1)	(2)
Generation (GWh)	-0.656***	-0.483**	0.151	0.077	-0.011	-0.013	-0.016	-0.014	-0.215	-0.274**
	(0.175)	(0.159)	(0.094)	(0.092)	(0.019)	(0.024)	(0.017)	(0.013)	(0.150)	(0.134)
Capacity factor	-0.021***	-0.014***	0.015**	0.012	0.047	0.018	-0.018	-0.006	-0.063***	-0.049***
	(0.003)	(0.003)	(0.006)	(0.007)	(0.041)	(0.064)	(0.012)	(0.011)	(0.009)	(0.009)
Obs.	1,915	1,915	1,915	1,915	910	910	1,915	1,915	1,915	1,915
Controls	×	×	×	×	×	×	×	×	×	×
τ_1 fixed effects	×		×		×		×		×	
τ_2 fixed effects		×		×		×		×		×

Notes: Marginal effects of 1 GWh of daily solar generation are derived from an OLS on daily aggregated generation, and from a fractional logit response model on daily capacity factors. Estimations include plants with both single- and dual-fuel engines. Controls include daily temperature, humidity, load and price ratios. Vector τ_1 includes year, month, and weekend fixed effects. Vector τ_2 includes year, seasons, year × seasons, and weekend fixed effects. Bootstrapped standard errors appear in parentheses. Significance levels: $^{*}p < 0.10$, $^{**}p < 0.05$, $^{***}p < 0.001$.

Table 5: The Effect of 1 GWh of Solar Generation on Daily Renewable Generation

	Wind		Hydro		Geothermal	
	(1)	(2)	(1)	(2)	(1)	(2)
Generation (GWh)	0.015	0.099***	-0.008***	-0.007***	-0.071***	-0.026
	(0.020)	(0.019)	(0.001)	(0.002)	(0.019)	(0.016)
Capacity factor	-0.004	0.013**	-0.021***	-0.018***	-0.050***	-0.040***
	(0.005)	(0.004)	(0.004)	(0.005)	(0.013)	(0.011)
Obs.	1,489	1,489	1,915	1,915	306	306
Controls	×	×	×	×	×	×
τ_1 fixed effects	×		×		×	
τ_2 fixed effects		×		×		×

Notes: Marginal effects of 1 GWh of daily solar generation are derived from an OLS on daily aggregated generation, and from a fractional logit response model on daily capacity factors. Estimations include plants with both single- and dual-fuel engines. Controls include daily temperature, humidity and load. Fuel price ratios are not included in this regression as these are renewable generators only. Vector τ_1 includes year, month, and weekend fixed effects. Vector τ_2 includes year, seasons, year × seasons, and weekend fixed effects. Bootstrapped standard errors appear in parentheses. Significance levels: $^{*}p < 0.10$, $^{**}p < 0.05$, $^{***}p < 0.001$.

solar generation reduces the day-to-day generation of plants running with coal and with natural gas by 0.48 and 0.27 GWh, respectively (columns 2).[25] Considering the descriptive statistics in Table 1, we observe that this displacement is roughly equivalent to 1.22% and 5.36% of the daily average power generated by these fossil fuels. Indeed, the results for capacity factors in Table 4 show qualitatively similar results. An extra 1 GWh of solar

[25]Further analysis using simple cycle turbine plants reveals that solar energy displaces coal-fired single-fuel engine generation at a larger magnitude (see Table A2 in the Appendix). This is an indication that the reduced coal use found in Table 4 is attenuated by dual-fuel engine coal-fired plants running with diesel.

generation displaces 1.4 percentage points of the capacity factors of plants running with coal, and 4.9 percentage points of the capacity factors of plants running with natural gas. Table 4 suggests a ramp-up on capacity factors of plants running with diesel. Yet, this effect disappears once a stronger set of time-fixed effects is included.

The results for renewables in Table 5 suggest similar displacement effects on hydro, a dispatchable power source. In particular, the results in columns (2) indicate that, on average, a 1 GWh increase in daily solar generation displaces hydro by 0.007 GWh, equivalent to 3.3% of the average hydro power generated in a single day. Regarding geothermal generation, we find no effects, although the results on capacity factors indicate a significant reduction of four percentage points. While this may be a weak effect, it is important to consider that the geothermal displacement attenuates the potential benefits of a reduction in fossil fuels found in 4. Because geothermal energy is a non-emitting source of electricity, its displacement will reduce some of the health benefits associated with the expansion of solar generation. Hydropower, on the other hand, is mostly utilized as a storage resource, dispatching in response to high price times; thus, we are unable to directly identify the environmental impacts of its displacement. Despite this potential attenuation, it is likely that the effect will be minor given the relatively small share of electricity that is produced by hydro and geothermal sources (0.4% and 0.4% of mean daily generation, respectively; see Table 1). In summary, we expect any attenuation effect from reduced hydro and geothermal generation to be small compared to the benefits of displaced coal and natural gas, which account for 83% and 11% of mean daily generation, respectively.

Finally, we find a positive coefficient of solar generation on wind generation, a non-dispatchable (but curtailable) power source. The result for wind in column (2) of Table 5 indicates that a 1 GWh of daily solar generation ramps up wind generation by 0.099 GWh. Due to the non-dispatchability of wind generation, this likely reflects an underlying correlation of wind and solar, given the thermally driven wind systems that characterize the Atacama Desert (Jacques-Coper et al., 2015). Thermally driven winds are caused by local differences in radiational heating and cooling systems, which in the case of the Atacama favor the complementarity between wind energy and solar energy (Jacques-Coper et al., 2015; Muñoz et al., 2018). An additional source of positive correlation between wind and solar generation may come from the country's effort to boost the adoption of renewable energy sources, which has encouraged the installation of several wind parks in addition to solar power plants (Ministry of Energy, 2013). In any case, given that wind generation is not dispatchable but is curtailable, the fact that we are not getting a negative coefficient weakly suggests that wind is not curtailed in response to greater solar output, or that, if curtailment

exists, it is not large enough to overcome the positive correlation between the two sources.

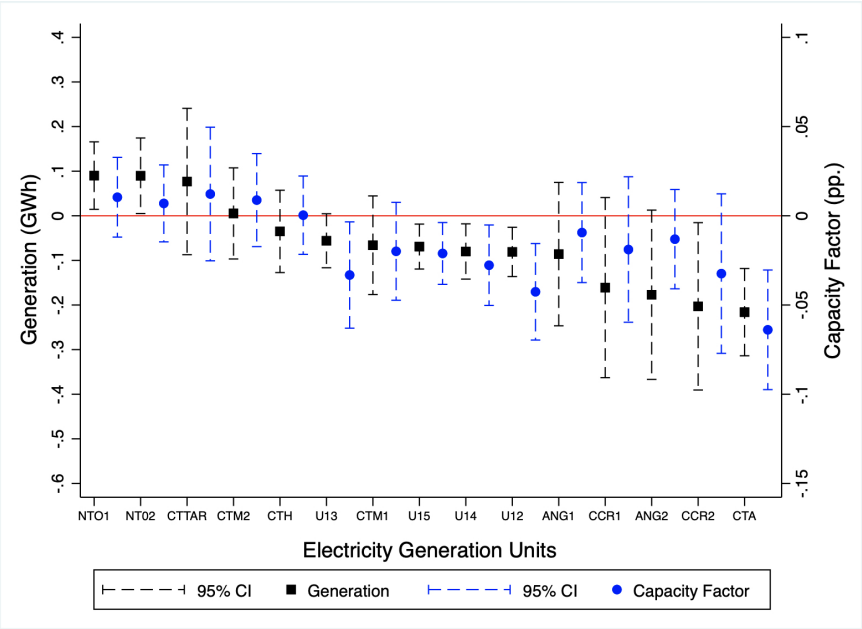

Figure 9: Coal-Fired EGUs and Displacement

Notes: The figure uses all EGUs that report coal (and its derivatives) as their primary fuel source. The left y-axis shows the marginal effects of 1 GWh of daily solar generation on plant-level daily generation using OLS. The right y-axis shows the marginal effects of 1 GWh of daily solar generation on daily capacity factors using a fractional logit response model. The estimation equation is identical to the one in columns (2) of Table 4. Dashed lines represent 95% confidence intervals obtained with bootstrapped standard errors.

To delve deeper into the displacement of fossil fuel EGUs indicated in Table 4, Figure 9 plots the marginal effect of solar generation on daily generation levels and capacity factors by coal-fired EGUs.[26] Squares represent the point estimate of solar generation on daily coal generation (left y-axis), and circles represent the marginal displacement of capacity factors (right y-axis). We observe that the negative impact of solar generation on coal combustion indicated in Table 4 is mostly explained by the shift in the generation of five units: U15, U14, U12, CCR2 and CTA. Figure 9 also reveals the displacement of unit U13, statistically significant at the 10% level. Four of these units (U15, U14, U13 and U12) are part of the Tocopilla coal-fired power station, which has been in operation since 1960 and is SING's oldest coal-fired plant.[27] The largest generation displacement is found for the CTA unit that belongs to the Atacama station. Power output for this unit decreased by 216 MWh, roughly equivalent to 7% of its capacity. Considering this plant alone, this displacement translates

[26]Similar graphs for diesel- and gas-fired units are provided in Figures A3 and A4, respectively, in the Appendix.

[27]At the time of writing, the Chilean government announced its plans to shut down these four units between 2019 and 2024. Source: Online. Retrieved: December 2019.

into more than 200 MWh of coal-fired generation avoided on a given day. This is closely followed by reductions in CCR2's output, one of the largest EGUs in the system (274.9 MW of gross capacity.[28] On average, our estimates reveal that 1 GWh of solar generation displaces 203 MWh of generation from the Atacama plant on a given day.

In addition to the displacement of several coal-fired units, Figure 9 also reveals a statistically significant ramp-up in the power generation of two facilities: NTO1 and NTO2. On average, 1 GWh of daily solar generation increases generation in these plants by 90 and 89 MWh, respectively, jointly equivalent to 0.46% of the daily coal-fired generation (see Table 1). These two units are part of the Norgener power plant, also located in Tocopilla. Although the ramp-up in the generation of these two coal-fired units is significantly lower than the displacement found for other facilities, the increase slightly attenuates the plausible health impact of the overall set of displaced plants in Tocopilla.

6.2 Solar Generation and Health Outcomes

The results on the effects of 1 GWh of solar generation on daily hospital admissions using Equation (3) are displayed in Table 6 for cardiovascular and respiratory conditions. We present these results using alternative groups of cities. Columns (1) and (2) both include controls that capture weather conditions, city-level mining production and demographics.[29] However, we vary the time-fixed effects across the two columns: columns (1) include year, month and weekend fixed effects, while columns (2) have more expansive time-fixed effects, including year, season, year season, and weekend fixed effects.

Altogether, the results indicate that solar generation leads to a reduction in hospital admissions. For the full sample, we observe that 1 GWh of solar generation leads to a 0.025 average reduction in daily hospital admissions due to cardiovascular conditions, and to a 0.06 average reduction in admissions due to all respiratory conditions (columns (2)). To the extent that emissions from displaced fossil fuel plants are not equally scattered across space, these results are likely underestimating the effect of solar energy. Thus, to better understand the effect of solar generation on health due to the displacement of emissions from dirty generators, we take into account the potential transport of pollutants and redefine our sample to include cities downwind of displaced fossil fuel plants.

With this subsample, we obtain a stronger and larger effect in general admissions due to

[28] Units CCR1 and CCR2 belong to the Cochrane Power Station, with more than 500 MW of gross capacity.

[29] It is important to control for mining production as this sector is a significant polluter in the area and the largest buyer of SING's power. See Section 5 for more details.

Table 6: The Effect of 1 GWh of Solar Generation on Hospital Admissions

	All Cities		Cities Downwind of Displaced Fossil Fuel Plants					
			$< 10km$		$< 50km$		$< 100km$	
	(1)	(2)	(1)	(2)	(1)	(2)	(1)	(2)
Panel A. Cardiovascular								
Solar	-0.003	-0.025*	-0.025	-0.061	-0.015	-0.037	-0.014	-0.022
	(0.013)	(0.014)	(0.048)	(0.070)	(0.091)	(0.040)	(0.021)	(0.015)
Panel B. All respiratory								
Solar	0.023	-0.060***	-0.087	-0.142**	-0.055	-0.092**	-0.037	-0.078
	(0.020)	(0.015)	(0.071)	(0.047)	(0.047)	(0.038)	(0.040)	(0.137)
Panel C. Upper respiratory								
Solar	-0.07	-0.021**	-0.037	-0.033***	-0.024**	-0.026***	-0.023**	-0.021
	(0.019)	(0.009)	(0.075)	(0.007)	(0.012)	(0.006)	(0.009)	(0.085)
Panel D. Lower respiratory								
Solar	0.022	-0.015	-0.064	-0.122***	0.005	-0.084***	-0.010	-0.067***
	(0.014)	(0.011)	(0.049)	(0.031)	(0.034)	(0.03)	(0.032)	(0.018)
Obs.	36,385	36,385	3,830	3,830	5,745	5,745	7,660	7,660
Controls	×	×	×	×	×	×	×	×
City fixed effects	×	×	×	×	×	×	×	×
τ_1 fixed effects	×		×		×		×	
τ_2 fixed effects		×		×		×		×

Notes: Marginal effects from ZINB panel-data regressions using 100 iterations. Inflate regressions at count zero are estimated using a logit estimator. Controls include weather, mining production, and demographic covariates (including population) in both the main and the inflate regressions. Vector τ_2 includes year, seasons, year × seasons, and weekend fixed effects. Clustered standard errors by city appear in parentheses. Significance levels: $^{*}p < 0.10$, $^{**}p < 0.05$, $^{***}p < 0.001$.

respiratory conditions in the immediate vicinity of displaced plants ($< 10km$), although we lose significance in cardiovascular conditions due to the reduction in statistical power. For cities within $10km$ downwind of displaced plants, we observe that 1 GWh of daily solar generation results in 0.142 fewer hospital admissions due to all respiratory diseases. Considering that daily solar-powered average electricity in our sample is equivalent to 1.46 GWh, these results indicate that solar generation has led to 76, 17 and 65 fewer annual hospital admissions due to all respiratory causes, upper respiratory diseases and lower respiratory diseases, respectively, in cities near displaced fossil fuel power plants ($< 10km$). Similar conclusions, albeit with decreasing magnitudes, are drawn for cities within $50km$ and $100km$ of distance from displaced facilities.

We repeat the estimation of Equations (3) and (4) for different age groups using our strongest specification (column (2) in Table 6). These results are given in Table 7 for all cities, and for cities downwind of and within $10km$ of displaced fossil fuel power plants. The results for cities downwind of displaced fossil fuel plants that are within $50km$ and $100km$ of their limits are presented in Table A3 in the Appendix.

Table 7: The Effect of 1 GWh of Solar Generation on Hospital Admissions by Age Group

	All Cities					Cities < 10km Downwind of Displaced Fossil Fuel Plants				
	Infants	Toddlers	Children	Adults	Seniors	Infants	Toddlers	Children	Adults	Seniors
Panel A. Cardiovascular										
Solar	-0.00003	-0.0004	-0.001	-0.013*	-0.004	-0.0003	-0.004	-0.001	-0.018	-0.020
	(0.002)	(0.036)	(0.002)	(0.008)	(0.012)	(0.001)	(0.014)	(0.006)	(0.048)	(0.028)
Panel B. All respiratory										
Solar	-0.020**	-0.010	-0.005	-0.005	-0.009***	-0.048	-0.033	-0.003	-0.012	-0.013**
	(0.007)	(0.011)	(0.007)	(0.005)	(0.002)	(0.092)	(0.034)	(0.456)	(0.082)	(0.006)
Panel C. Upper respiratory										
Solar	-0.0001	-0.002	-0.011**	-0.007*	-0.001	-0.0001	-0.011	-0.005	-0.002	-0.001
	(0.001)	(0.004)	(0.005)	(0.004)	(0.001)	(0.011)	(0.144)	(0.011)	(0.059)	(0.006)
Panel D. Lower respiratory										
Solar	-0.012	-0.006	0.002	0.001	-0.002	-0.044	-0.022	-0.005	-0.008	-0.014
	(0.012)	(0.005)	(0.009)	(0.006)	(0.004)	(0.086)	(0.065)	(0.135)	(0.134)	(0.080)
Obs.	36,385	36,385	36,385	36,385	36,385	3,830	3,830	3,830	3,830	3,830
Controls	×	×	×	×	×	×	×	×	×	×
City fixed effects	×	×	×	×	×	×	×	×	×	×
τ_2 fixed effects	×	×	×	×	×	×	×	×	×	×

Notes: Marginal effects from ZINB panel-data regressions using 100 iterations. Inflate regressions at count zero are estimated using a logit estimator. Controls include weather, mining production and demographic covariates (including population) in both the main and the inflate regressions. Vector τ_2 includes year, seasons, year × seasons, and weekend fixed effects. Clustered standard errors by city appear in parentheses. Significance levels: $^{*}p < 0.10$, $^{**}p < 0.05$, $^{***}p < 0.001$.

The results suggest that solar generation, through the displacement of fossil fuel energy, leads to a positive effect in health outcomes across most age groups. Because we show the results here for a limited sample of downwind cities, the number of observations in each age group is significantly limited, thereby restricting the power of our estimation and reducing the statistical significance. Thus, this regression of downwind cities identifies only statistically significant improvements in all respiratory hospitalizations for seniors. However, when we expand the buffer up to a distance of within 100km of a displaced fossil fuel plant, we find reductions in respiratory hospitalizations for toddlers, children and seniors. We still do not identify any statistically significant impact on cardiovascular hospitalizations.

6.2.1 Long-Term Health Effects

The results in Table 6 offer a general perspective of the net effect that day-to-day variation in solar generation has on day-to-day variation in hospital admissions. Additional evidence of the immediate co-benefit of solar is found in the results for Infants in Table 7, and in Table A3. As stated in Currie and Neidell (2005), the link between cause and effect is immediate in the case of infants, whereas diseases today in adults may reflect pollution exposure from years ago. This immediate link is illustrated by the negative and statistically

significant effect of solar generation on hospital admissions of infants due to all respiratory diseases found in panel B of Table 7. Comparable effects are found in panels B and D of Table A3. Considering that infants are less than one year old, these findings corroborate the contemporaneous aspect of the co-benefits of solar power generation.

To test whether these co-benefits also mask some permanent effects, we use the estimation of Equation (4) where main explanatory variable is allowed to reflect the moving weekly, monthly or yearly average solar generation in the system. Equation (4) also allows us to take into account potential lagged effects of solar generation on contemporaneous health outcomes, albeit indirectly. To that end, we express $S = S_t$, where $t = \{w, m, y\}$. Modeled in this way, δ_t gives us the average marginal effect of 1 GWh of either weekly, monthly or yearly average generation on daily relevant hospitalizations. The results using our strongest specification are depicted in Table 8 for all ages, and in Table A5 by age group.

Table 8: The Long-Term Effect of 1 GWh of Solar Generation on Daily Hospital Admissions

	All Cities			Cities Downwind of Displaced Fossil Fuel Plants								
				$< 10km$			$< 50km$			$< 100km$		
	t=week	t=month	t=year	t=week	t=month	t=year	t=week	t=month	t=year	t=week	t=month	t=year
Panel A. Cardiovascular												
Solar$_t$	-0.043**	-0.058	-0.097**	-0.078	-0.112	-0.216	-0.050	-0.073	-0.146*	-0.031*	-0.034	-0.046
	(0.015)	(0.178)	(0.036)	(0.104)	(0.118)	(0.150)	(0.057)	(0.052)	(0.083)	(0.019)	(0.035)	(0.074)
Panel B. All respiratory												
Solar$_t$	-0.090***	-0.054**	-0.026	-0.177**	-0.084**	0.068	-0.116**	-0.055	0.041	-0.094**	-0.052**	0.024
	(0.014)	(0.018)	(0.044)	(0.067)	(0.027)	(0.049)	(0.039)	(0.056)	(0.027)	(0.036)	(0.024)	(0.016)
Panel C. Upper respiratory												
Solar$_t$	-0.019	-0.019	-0.022	-0.046***	-0.016	0.011	-0.030	-0.013	-0.0002	-0.025**	-0.014	-0.004
	(0.012)	(0.019)	(0.025)	(0.010)	(0.038)	(0.043)	(0.019)	(0.427)	(0.029)	(0.010)	(0.145)	(0.198)
Panel D. Lower respiratory												
Solar$_t$	-0.016	-0.005	0.009	-0.137*	-0.073	0.067	-0.101**	-0.056	0.032	-0.081**	-0.046	0.024
	(0.017)	(0.015)	(0.034)	(0.071)	(0.091)	(0.127)	(0.044)	(0.052)	(0.080)	(0.035)	(0.042)	(0.054)
Obs.	36,366	36,366	36,366	3,828	3,828	3,828	5,742	5,742	5,742	7,656	7,656	7,656
Controls	×	×	×	×	×	×	×	×	×	×	×	×
City fixed effects	×	×	×	×	×	×	×	×	×	×	×	×
τ_2 fixed effects	×	×	×	×	×	×	×	×	×	×	×	×

Notes: Marginal effects from ZINB panel-data regressions using 100 iterations. Inflate regressions at count zero are estimated using a logit estimator. Controls include weather, mining production and demographic covariates (including population) in both the main and the inflate regressions. Vector τ_2 includes year, seasons, year × seasons, and weekend fixed effects. Clustered standard errors by city appear in parentheses. Significance levels: $^{*}p < 0.10$, $^{**}p < 0.05$, $^{***}p < 0.001$.

The results in Table 8 show the largest reductions in hospitalizations from weekly average generation relative to those in columns (2) of Table 6, particularly for cities downwind of nearby fossil fuel plants ($< 10km$). The fact that this coefficient is slightly greater than the daily impact as reported in Table 6 suggests an additional effect of reduced cumulative pollution exposure, although this added effect is present only in the relatively short term. These cumulative effects, however, seem to be present in the relatively short term only, as they become smaller and generally less significant as we move toward longer times of

exposure (monthly and yearly).

When exploring the results by age group in Table A5, we observe reductions in hospital admissions of infants, children and seniors from weekly average generation. For instance, for this last age group living in cities downwind of nearby thermal generation plants ($< 10km$), we observe a significant reduction of 0.025 in daily hospital admissions due to lower respiratory diseases from weekly solar generation. Comparing this to the results in Table 7, we observe that the health effect of weekly solar generation for this age group is in line with the presence of some cumulative effects but only in the short term, as it is significantly greater than the effect of daily variation in solar power. Similar conclusions can be drawn for infants and children. Taken together, the results in Tables 8 and A5 suggest that the average health effects of exposure to reduced fossil fuel pollution are largely contemporaneous rather than cumulative.

6.2.2 Fossil Fuel Generation, Pollution and Health in Chilean Cities

Our previous health results consistently show significant reductions in pollution-related hospital admissions due to variation in solar power generation in Chile. Additionally, these reductions are found mostly in cities downwind of fossil fuel plants that are displaced by solar generation as revealed by our plant-level displacement analysis. While this strategy helps us to take into account the air transport of pollutants emitted by thermal plants affected by the injection of new solar power generation into the grid, it constitutes an indirect test of the mechanism through which solar generation affects health. In this section, we explore a more direct test on the mechanism through which solar generation is positively affecting pollution-related admissions by using available data on $PM_{2.5}$ concentrations for some of the cities in our sample. As mentioned in Section 3.1.2, pollution data in Chile is scarce for cities other than Santiago, yet we are able to gather data for some of the cities with fossil fuel generation, and cities downwind of displaced fossil fuel plants.[30] With these data, we first test the link between thermal generation and air pollution concentrations, estimating the effect of daily fossil fuel generation (i.e., coal, diesel and natural gas) on daily $PM_{2.5}$ concentrations (in logs) as follows:

$$\log(PM_{2.5})_{jd} = \rho_0 + \rho_1 Coal_{jd} + \rho_2 Diesel_{jd} + \rho_3 NaturalGas_{jd} + \omega_{jd} + \zeta + \tau + \upsilon_{jd}, \quad (5)$$

[30]Specifically, we have data for Arica, Antofagasta, Tocopilla and Alto Hospicio. The last two cities, namely Tocopilla and Alto Hospicio, are part of the group of cities within $10km$ downwind of displaced fossil fuel plants. Pollution data was gathered from https://sinca.mma.gob.cl.

where ω_{jd} is a vector of daily city-level weather covariates (including wind speed, also available for these cities); ζ is a vector of demographics, mining production and city-fixed effects; τ is a vector of time-fixed effects; and υ_{jd} is an idiosyncratic error. In an alternative specification, we replace thermal power for system-level daily solar generation. We estimate Equation (5) with OLS using Newey–West standard errors to control for potential autocorrelation known to affect pollution data.

Table 9: The Effect of 1 GWh of Power Generation on Daily Log $PM_{2.5}$

	All Cities				Cities < $10km$ Downwind of Displaced Fossil Fuel Plants			
	(1)	(2)	(1)	(2)	(1)	(2)	(1)	(2)
Coal	0.007	0.014**			0.011**	0.020***		
	(0.005)	(0.005)			(0.005)	(0.006)		
Diesel	-0.043	0.091			-0.138	-0.003		
	(0.105)	(0.104)			(0.126)	(0.123)		
Natural Gas	0.006	0.009			0.009	0.011*		
	(0.005)	(0.06)			(0.006)	(0.006)		
Solar			0.007	-0.033**			-0.019	-0.043**
			(0.013)	(0.013)			(0.016)	(0.019)
Obs.	5,582	5,582	5,319	5,319	2,592	2,592	2,329	2,329
Controls	×	×	×	×	×	×	×	×
City fixed effects	×	×	×	×	×	×	×	×
τ_1 fixed effects	×		×		×		×	
τ_2 fixed effects		×		×		×		×

Notes: Marginal effects from an OLS regression using Newey–West standard errors (in parentheses) allowing for up to three lags. Controls include weather (min. and max. temperature, humidity and wind speed), mining production and demographic covariates (including population). Vector τ_1 includes year, month, and weekend fixed effects. Vector τ_2 includes year, seasons, year × seasons, and weekend fixed effects. Significance levels: $^{*}p < 0.10$, $^{**}p < 0.05$, $^{***}p < 0.001$.

The results for the strongest specification in columns (2) of Table 9 show that 1 GWh of coal-fired generation increases $PM_{2.5}$ concentrations by 1% in all cities for which we have data. This effect becomes stronger and highly significant when looking at cities downwind of fossil fuel plants. Specifically, 1 GWh of coal generation increases concentrations of $PM_{2.5}$ by 2%, while 1 GWh of natural gas generation does so by 1%.[31] Considering that daily average concentrations of this pollutant are roughly 14.73 $\mu g/m^3$ across cities with data, these effects are equivalent to 0.295 and 0.147 $\mu g/m^3$ daily increases in $PM_{2.5}$. These results are consistent with our previous findings on the displacement of coal-fired and gas-fired facilities. Yet, they should be taken with caution as they cover the period between 2012 and 2017, already treated with the injection of solar generation, which may explain the reduced

[31] As mentioned in our displacement analysis, all gas-fired plants in our sample are combined-cycled plants that operate with diesel as well, so this effect is likely due to the use of diesel in gas-fired plants.

magnitude of the coefficients. When replacing thermal generation with solar generation, we find consistent and significant results. The results in columns (2) of Table 4 indicate that 1 GWh of solar generation reduces $PM_{2.5}$ concentrations by 3–4%. Altogether, the findings in Table 4 indicate that thermal generation effectively increases airborne pollution concentrations, while solar generation has the opposite effect.

Our final exercise considers the information in Table 4 in tandem with our health analysis. To that end, we follow two approaches. First, we re-estimate our baseline ZINB health equations, replacing the solar generation variable with city-level daily average $PM_{2.5}$ concentrations. In doing this, we have to consider that pollution-related hospital admissions are likely not orthogonal to $PM_{2.5}$ concentrations. For instance, $PM_{2.5}$ can be formed due to chemical reactions of secondary particles from SO_2 and NO_X, pollutants that are also common to coal combustion and have a direct impact on health as well (World Health Organization, 2006). In addition, other factors such as economic conditions may have a simultaneous impact on both health outcomes and air pollution concentrations. Thus, while informative, omitted factors in this regression may give us an inconsistent estimate of the impacts of pollution on health.

The results on the health effects of $PM_{2.5}$ are depicted in the ZINB column in Table 10 for all cities and downwind cities. In line with our previous analyses, we observe that 1 $\mu g/m^3$ of $PM_{2.5}$ concentrations increases daily lower respiratory admissions in all cities, and all respiratory and lower respiratory admissions in downwind cities. We also observe counterintuitive, negative results for cardiovascular admissions in downwind cities, a result plausibly explained by the endogeneity of our main explanatory variable. We solve this issue in a second strategy, in which we use day-to-day variation in solar generation in an instrumental variable approach that uses a control function (CF) estimation (Wooldridge, 2015). We adopt this two-step estimation given the non-linear distribution of the dependent variable in the health equations, our second-stage equations.[32] We carry out this CF exercise using Equation (5) (unlogged) in a first-stage estimation with solar generation as the instrument, and computing the residuals $\hat{v}_{jd}$ that we include as an additional regressor in the estimation of Equation (3) that uses $PM_{2.5}$ as the main explanatory variable. A statistically significant second-stage control function coefficient $\hat{v}_{jd}$ constitutes a simple test on the endogeneity of $PM_{2.5}$ (Wooldridge, 2010), and can be interpreted as the effect of solar on health outcomes through reductions in $PM_{2.5}$. We present these results in column CF of Table 10, with bootstrapped standard errors.

Daily variation in $PM_{2.5}$ is found to increase daily respiratory admissions for all cities in our

[32]See E.G., Kline and Walters (2016) for a recent example on the use of a control function approach.

Table 10: The Effect of Daily $PM_{2.5}$ on Daily Hospital Admissions

	All Cities		Cities < 10km Downwind of Displaced Fossil Fuel Plants	
	ZINB	CF	ZINB	CF
Panel A. Cardiovascular				
$PM_{2.5}$	-0.003	-0.006	-0.001***	0.020
	(0.007)	(0.023)	(0.0004)	(0.021)
$\hat{v}$		0.005		-0.023
		(0.024)		(0.022)
Panel B. All respiratory				
$PM_{2.5}$	0.008	0.053**	0.009***	0.073*
	(0.009)	(0.021)	(0.002)	(0.041)
$\hat{v}$		-0.050**		-0.069*
		(0.021)		(0.042)
Panel C. Upper respiratory				
$PM_{2.5}$	-0.002	0.002	0.002	0.005
	(0.006)	(0.011)	(0.002)	(0.017)
$\hat{v}$		-0.006		-0.003
		(0.014)		(0.012)
Panel D. Lower respiratory				
$PM_{2.5}$	0.012***	0.034	0.007**	0.059**
	(0.004)	(0.029)	(0.003)	(0.021)
$\hat{v}$		-0.024		-0.054**
		(0.027)		(0.021)
First Stage ($Solar_d$)		-0.600***		-0.900***
		(0.120)		(0.232)
Obs.	5,319	5,319	2,329	2,329
Controls	×	×	×	×
City fixed effects	×	×	×	×
τ_2 fixed effects	×	×	×	×

Notes: Marginal effects from both ZINB and CF ZINB regressions. $PM_{2.5}$ is measured in $\mu g/m^3$. $\hat{v}$ are the residuals from the estimation of Equation (5). Controls include weather (min and max temperature, humidity and wind speed), mining production and demographic covariates (including population). Vector τ_2 includes year, seasons, year × seasons, and weekend fixed effects. Clustered standard errors by city (ZINB) and boostrapped standard errors (CF) appear in parentheses. Significance levels: $^{*}p < 0.10$, $^{**}p < 0.05$, $^{***}p < 0.001$.

sample. Additionally, a statistically significant estimate for $\hat{v}_{jd}$ corroborates the endogeneity of $PM_{2.5}$, which may explain the lack of significance of this estimate in the previous ZINB regression, or its counterintuitive signs. In fact, the negative $\hat{v}_{jd}$ coefficient suggests that solar generation effectively reduces the impact of $PM_{2.5}$ on all hospital admissions, particularly all respiratory admissions. We find consistent results when restricting the sample to downwind cities. In this case, the CF results indicate a positive effect of $PM_{2.5}$ on daily respiratory and lower respiratory admissions, results that are almost fully mitigated by the injection of solar generation. We take the results in Tables 9 and 10 as strong evidence that the co-benefits of solar power generation on hospital admissions found throughout our analysis are largely due to reductions in airborne pollution from displaced thermal generation.

7 Robustness Checks

7.1 Alternative Groups of Cities

Our results are robust to several alternative specifications. First, we check the robustness of our wind direction analysis by splitting the sample between cities with and without fossil fuel plants as an approximation to cities with and without pollution exposure. From our displacement analysis, we are also able to consider cities that are downwind of fossil fuel plants that were not displaced by the addition of solar generation into the grid, and cities upwind of the displaced ones. We present these results in Table 11 using our strongest specification.

Table 11: The Effect of 1 GWh of Solar Generation on Health Using Alternative Cities

	With Fossil Fuel Generation	Without Fossil Fuel Generation	Downwind of Nondisplaced Fossil Fuel Plants	Upwind of Nondisplaced Fossil Fuel Plants
Panel A. Cardiovascular				
Solar	-0.051	-0.015	0.007**	-0.0003
	(0.054)	(0.010)	(0.003)	(0.002)
Panel B. All respiratory				
Solar	-0.215*	-0.023	-0.025	-0.002
	(0.127)	(0.021)	(0.076)	(0.005)
Panel C. Upper respiratory				
Solar	-0.093	-0.005	-0.003	-0.0002
	(0.166)	(0.006)	(0.007)	(0.003)
Panel D. Lower respiratory				
Solar	-0.111***	-0.007	-0.008	0.001
	(0.029)	(0.008)	(0.165)	(0.002)
Obs.	9,575	24,895	3,830	7,660
Controls	×	×	×	×
City Fixed Effects	×	×	×	×
τ_2	×	×	×	×

Notes: Marginal effects from ZINB panel-data regressions using 100 iterations. All regressions include weather covariates, season, year, weekend, city-fixed effects, demographics (e.g., density, fertility rate and poverty rate) and mining production, in both the main and the inflate regressions. Inflate regressions at count zero are estimated using a logit estimator. Clustered standard errors by city appear in parentheses. Significance levels: $^{*}p < 0.10$, $^{**}p < 0.05$, $^{***}p < 0.001$.

Splitting the sample in this manner reveals that reductions in hospitalizations attributable to solar generation are primarily found in places with fossil fuel generation. The results in the first two columns of Table 11 suggest that additional solar generation predominantly curtails lower respiratory admissions in cities where displacement is possible. Namely, an additional 1 GWh of solar generation results in 0.111 fewer daily lower respiratory admissions in cities that house fossil fuel plants, roughly equivalent to 59 fewer yearly hospitalizations.

We do not find a statistically significant impact on hospitalizations for upper respiratory or cardiovascular-related conditions, likely due to the failure to account for pollution transport. We do find, however, a small but positive significant impact on cardiovascular hospitalizations in cities downwind of nondisplaced fossil fuel plants. Namely, a 1 GWh of solar generation is found to increase by 0.007 the number of daily hospital admissions due to cardiovascular diseases. This is certainly an unexpected result, but it is important to point out that this subsample includes only two cities, Sierra Gorda and Mejillones, and that the latter hosts all gas-fired plants. Although our aggregated displacement analysis reveals that solar generation displaces gas-fired generation, our plant-level analysis shows that one gas-fired unit ramps up its production in response to the injection of this renewable (see Figure A4 in the Appendix). Thus, a plausible explanation is that some pollution from this power plant reaches parts of this city, even though it is downwind of nondisplaced plants. While we do not explore this possibility further in the paper, it is important to note that this effect is small in magnitude relative to those for cities with fossil fuel generation.[33] Finally, and in contrast to our findings in Table 6 for downwind cities, we find no statistically significant effects in cities upwind of displaced fossil fuel plants.

7.2 Rate of Hospital Admissions

We also estimate an alternative version of our health equation using the rate of hospital admissions per 100,000 people as the outcome variable. We present the OLS results for our strongest health specification in Table 12. We find similar magnitudes of reduced hospitalizations across all cities, although we lose significance when subsampling to downwind cities alone. Here, it is important to consider that we have many small cities in our sample, which translates into an abundant number of observations with zero daily hospital admissions. Ideally, our OLS estimations using rate of admissions would account for this large number of zeros in the data, yet that is not the case. While the OLS results on the rate of admissions in Table 12 are useful as a first approximation, we take them with caution given the skewed distribution of this dependent variable.

[33] We cannot estimate our health equations for cities downwind of the few plants ramping up their generation in response to solar generation because, simultaneously, these cities are also downwind of some displaced fossil fuel plants.

Table 12: The Effect of 1 GWh of Solar Generation on the Rate of Hospital Admissions

	All Cities	Cities Downwind of Displaced Fossil Fuel Plants		
		$< 10km$	$< 50km$	$< 100km$
Panel A. Cardiovascular				
Solar	-0.004	-0.042	-0.043	-0.020
	(0.041)	(0.116)	(0.065)	(0.048)
Panel B. All respiratory				
Solar	-0.116**	-0.329	-0.192	-0.253
	(0.054)	(0.273)	(0.201)	(0.154)
Panel C. Upper respiratory				
Solar	-0.027	-0.078	-0.044	-0.053
	(0.020)	(0.065)	(0.045)	(0.032)
Panel D. Lower respiratory				
Solar	-0.086**	-0.269	-0.160	-0.193
	(0.041)	(0.232)	(0.169)	(0.122)
Obs.	36,328	3,824	5,736	7,648
Controls	×	×	×	×
City Fixed Effects	×	×	×	×
τ_2	×	×	×	×

Notes: Marginal effects from OLS panel-data regressions. Controls include weather, mining production and demographic covariates (including population) in both the main and the inflate regressions. Vector τ_2 includes year, seasons, year × seasons, and weekend fixed effects. Clustered standard errors by city appear in parentheses. Significance levels: $^{*}p < 0.10$, $^{**}p < 0.05$, $^{***}p < 0.001$.

7.3 Placebo Health Outcomes

Additionally, we test whether solar generation affects health outcomes that are, presumably, unrelated to pollution. Table 13 displays the ZINB results of this falsification test using infections(panel A), type 1 diabetes (panel B) and blood diseases (excluding anemia) (panel C). We also include Schlenker and Walker (2016)'s placebo outcomes: strokes (panel D), bone fractures (panel E) and appendicitis (panel F).[34] The placebo results are all small and statistically insignificant, regardless of the group of cities considered, except for appendicitis, which has a positive effect at $50km$ downwind of displaced plants. This is not a peculiar result given the findings in Guidetti et al. (2020) and the potential hospital capacity constraints experienced by developing countries. Whether or not spikes in pollution displace admissions due to other conditions in strained hospitals, a reduction in pollution-related admissions may increase hospitalizations for other procedures such as appendicitis. This possibility remains an open avenue for future research.

[34]The exact International Classification of Diseases (ICD)-10 codes are [A00,A099] and [B50,B999] for intestinal, protozoal, worm and other infectious diseases; [E100,E149] for type 1 diabetes mellitus; [D70,D899] for blood disorders; [I64,I679] for strokes; [S000,S929] for bone fractures; and [K352,K389] for appendicitis.

Table 13: The Effect of 1 GWh of Solar Generation on Placebo Outcomes

	All	Cities Downwind of Displaced Fossil Fuel Plants		
	Cities	$< 10km$	$< 50km$	$< 100km$
Panel A. Infections				
Solar	-0.005	-0.010	-0.008	-0.008
	(0.006)	(1.623)	(0.017)	(0.080)
Panel B. Type 1 Diabetes				
Solar	-0.005	-0.032	-0.020	-0.015
	(0.005)	(0.113)	(0.015)	(0.025)
Panel C. Blood-Related Diseases				
Solar	-0.0004	0.002	0.0007	0.001
	(0.007)	(0.010)	(0.005)	(0.002)
Panel D. Strokes				
Solar	0.001	0.003	0.001	0.0001
	(0.004)	(0.007)	(0.003)	(0.002)
Panel E. Bone Fractures				
Solar	-0.016	0.003	0.0005	-0.001
	(0.019)	(0.022)	(0.013)	(0.011)
Panel F. Appendicitis				
Solar	-0.012	0.026	0.037^{***}	0.022
	(0.011)	(0.023)	(0.008)	(0.084)
Obs.	36,385	3,830	5,745	7,660
Controls	×	×	×	×
City fixed effects	×	×	×	×
τ_2 fixed effects	×	×	×	×

Notes: Marginal effects from ZINB panel-data regressions using 100 iterations. All regressions include weather covariates, season, year, weekend, city-fixed effects, demographics (e.g., density, fertility rate and poverty rate) and mining production, in both the main and the inflate regressions. Clustered standard errors by city appear in parentheses. Significance levels: $^{*}p < 0.10$, $^{**}p < 0.05$, $^{***}p < 0.001$.

8 Discussion

The remarkable and rapid expansion of solar generation capacity in Chile has provided a natural experiment to test the impact of renewable electricity sources on morbidity in a developing country. We run a variety of different tests to quantify the health benefits of almost 600 MW of new solar generation capacity. Overall, our results tell a positive story about how we can employ solar energy to bring about improved health outcomes in settings with elevated pollution exposure and reduced healthcare access.

We first demonstrate that solar energy can effectively displace fossil fuel plants, notably plants that rely on coal and natural gas. These heavy emitters are displaced by increases in solar generation, although the benefits may be attenuated by reductions in hydro and geothermal electricity. However, given the relatively small shares of these fuel types in generation, the attenuation of displacement is not enough to offset the positive health benefits.

We next show that the day-to-day operation of solar plants reduces daily hospitalizations

of cardiovascular and respiratory diseases, particularly those related to the upper airways. When taking into account the transport of pollutants using cities downwind of fossil fuel plants displaced by solar generation, we find significant morbidity reductions associated with all types of respiratory diseases, noticeable up to 50 km from the displaced facilities, and up to 100 km in the case of lower respiratory diseases. Although all ages are affected by this, we find higher reductions in hospitalizations of infants, children and seniors, the most vulnerable age groups. A simple linear projection of our results suggests that a full solar displacement of all coal-fired generation in the current grid would imply 287 and 129 fewer respiratory admissions of infants and seniors per year, respectively.[35] In the case of infants, this number scales up to 445 fewer respiratory admissions in cities downwind of displaced thermal plants. Furthermore, we show that the health co-benefits of solar generation are mainly contemporaneous, and are primarily located in cities downwind of displaced plants and those hosting fossil fuel generation. This demonstrates the geographic heterogeneous effect of solar generation, and simultaneously suggests that areas with intense fossil fuel generation will benefit more from an expansion of renewable, clean energy sources.

Our results remain unaltered after using several robustness checks, which include the use of cities without thermal generation, upwind cities and cities downwind of nondisplaced plants. Although our results are also robust to using hospital admissions due to other conditions presumably not related to pollution, we find a significant increase in appendicitis admissions, which may be related to a temporary alleviation of otherwise strained hospitals — a common characteristic in developing countries. This possibility remains an open question for future research.

Our study provides important evidence that solar generation can bring about positive health outcomes in developing nations, increasing the social benefits of investment in power generation capacity for these clean resources. To the extent that these countries suffer from limited healthcare infrastructure that forces them to adjust their healthcare needs during spikes in air pollution (Guidetti et al., 2020), or that their poor populations may be more likely to be exposed to pollution, our results should be considered as a lower bound of the true co-benefits that solar generation can bring to developing countries.

This work can be improved in several ways. Ideally, patient location would be used to determine their exact proximity to the polluting source. As we lack individual- or household-level data, our results represent a health outcome averaged across all individuals located in the same city. Future research could closely explore heterogeneous impacts of renewable

[35] Infants: 0.02×39.36 GWh (average daily coal-fired generation) $\times 365 = 287$. Seniors: 0.009×39.36 GWh (average daily coal-fired generation) $\times 365 = 129$.

generation considering different intensities in exposures to the polluting source. Additionally, we lack comprehensive data to explore the impact of solar power generation on global and other airborne emissions beyond $PM_{2.5}$. Furthermore, our work estimates the impact of solar generation prior to the northern and southern grid interconnection in Chile; identifying the effect once these two grids are interconnected is another potential avenue of research outside the scope of this paper.[36] Finally, complementary insights on the health benefits of renewable sources can be drawn from other health outcomes as well, such as mortality data. These avenues remain open topics for future research.

References

Abel, D., Holloway, T., Harkey, M., Rrushaj, A., Brinkman, G., Duran, P., Janssen, M., and Denholm, P. (2018). Potential air quality benefits from increased solar photovoltaic electricity generation in the eastern united states. *Atmospheric Environment*, 175:65–74.

Anenberg, S. C., Schwartz, J., Shindell, D., Amann, M., Faluvegi, G., Klimont, Z., Janssens-Maenhout, G., Pozzoli, L., Van Dingenen, R., Vignati, E., et al. (2012). Global air quality and health co-benefits of mitigating near-term climate change through methane and black carbon emission controls. *Environmental health perspectives*, 120(6):831–839.

Arceo, E., Hanna, R., and Oliva, P. (2016). Does the Effect of Pollution on Infant Mortality Differ Between Developing and Developed Countries? Evidence from Mexico City. *The Economic Journal*, 126(591):257–280.

Baker, E., Fowlie, M., Lemoine, D., and Reynolds, S. S. (2013). The economics of solar electricity.

Banzhaf, S., Ma, L., and Timmins, C. (2019). Environmental justice: The economics of race, place, and pollution. *Journal of Economic Perspectives*, 33(1):185–208.

Barbose, G., Wiser, R., Heeter, J., Mai, T., Bird, L., Bolinger, M., Carpenter, A., Heath, G., Keyser, D., Macknick, J., et al. (2016). A retrospective analysis of benefits and impacts of us renewable portfolio standards. *Energy Policy*, 96:645–660.

[36] The *a priori* effect of the interconnection on the health benefits of solar generation is unclear, due to two factors. First, although Chile's major population centers are in the south, which would imply greater impacts from solar generation on health, solar generation is more likely to occur in the north, given the region's massive solar irradiation compared to southern Chile. Thus, transmission constraints would likely attenuate that benefit. Second, because the southern grid is cleaner, the relative benefits of solar generation will be lower compared to that in northern Chile.

Barrows, G., Garg, T., and Jha, A. (2018). The economic benefits versus environmental costs of india's coal-fired power plants. *Available at SSRN*.

Bateson, T. F. and Schwartz, J. (2007). Children's Response to Air Pollutants. *Journal of Toxicology and Environmental Health, Part A*, 71(3):238–243.

Bell, M. L., Dominici, F., and Samet, J. M. (2005). A Meta-Analysis of Time-Series Studies of Ozone and Mortality With Comparison to the National Morbidity, Mortality, and Air Pollution Study. *Epidemiology*, 16(4):436–445.

Bell, M. L., McDermott, A., Zeger, S. L., Samet, J. M., and Dominici, F. (2004). Ozone and Short-term Mortality in 95 US Urban Communities, 1987-2000. *JAMA*, 292(19):2372–2378.

Brook, R. D., Rajagopalan, S., Pope III, C. A., Brook, J. R., Bhatnagar, A., Diez-Roux, A. V., Holguin, F., Hong, Y., Luepker, R. V., Mittleman, M. A., et al. (2010). Particulate matter air pollution and cardiovascular disease: an update to the scientific statement from the american heart association. *Circulation*, 121(21):2331–2378.

Buonocore, J. J., Luckow, P., Norris, G., Spengler, J. D., Biewald, B., Fisher, J., and Levy, J. I. (2016). Health and Climate Benefits of Different Energy-Efficiency and Renewable Energy Choices. *Nature Climate Change*, 6(1):100–105.

Burney, J. A. (2020). The downstream air pollution impacts of the transition from coal to natural gas in the united states. *Nature Sustainability*, pages 1–9.

Callaway, D. S., Fowlie, M., and McCormick, G. (2018). Location, Location, Location: The Variable Value of Renewable Energy and Demand-Side Efficiency Resources. *Journal of the Association of Environmental and Resource Economists*, 5(1):39–75.

Carlson, C. L. and Adriano, D. C. (1993). Environmental Impacts of Coal Combustion Residues. *Journal of Environmental quality*, 22(2):227–247.

Casey, J. A., Gemmill, A., Karasek, D., Ogburn, E. L., Goin, D. E., and Morello-Frosch, R. (2018a). Increase in fertility following coal and oil power plant retirements in california. *Environmental Health*, 17(1):44.

Casey, J. A., Karasek, D., Ogburn, E. L., Goin, D. E., Dang, K., Braveman, P. A., and Morello-Frosch, R. (2018b). Retirements of coal and oil power plants in california: association with reduced preterm birth among populations nearby. *American journal of epidemiology*, 187(8):1586–1594.

Chauhan, A. J., Inskip, H. M., Linaker, C. H., Smith, S., Schreiber, J., Johnston, S. L., and

Holgate, S. T. (2003). Personal exposure to nitrogen dioxide (NO2) and the severity of virus-induced asthma in children. *The Lancet*, 361(9373):1939–1944.

Chay, K. Y. and Greenstone, M. (2003a). Air Quality, Infant Mortality, and the Clean Air Act of 1970. Technical report, National Bureau of Economic Research.

Chay, K. Y. and Greenstone, M. (2003b). The Impact of Air Pollution on Infant Mortality: Evidence from Geographic Variation in Pollution Shocks Induced by a Recession. *The Quarterly Journal of Economics*, 118(3):1121–1167.

Chen, Y., Ebenstein, A., Greenstone, M., and Li, H. (2013). Evidence on the Impact of Sustained Exposure to Air Pollution on Life Expectancy from China's Huai River Policy. *Proceedings of the National Academy of Sciences of the United States of America*, 110(32):12936–12941.

Chile Environmental Ministry (2017). Informe Consolidado de Emisiones y Transferencia de Contaminantes 2005-2017. Retrieved from RETC, Ministerio de Medio Ambiente: ttps://retc.mma.gob.cl.

Chile Environmental Ministry (2018). Tercer Informe Bienal de Actualización de Chile sobre Cambio Climático. Retrieved from Ministerio de Medio Ambiente: https://www.mma.gob.cl.

Clarkson, T. W. (1990). Mercury – An Element of Mystery. *The New England Journal of Medicine*, 323(16):1137–1139.

Comisión Nacional de Energía (2018). Anuario Estadístico de Energía. Retrieved from Comisión Nacional de Energía: https://www.cne.cl.

Coneus, K. and Spiess, C. K. (2010). Pollution exposure and infant health: Evidence from germany.

Cullen, J. (2013). Measuring the Environmental Benefits of Wind-Generated Electricity. *American Economic Journal: Economic Policy*, 5(4):107–33.

Cullen, J. A. and Mansur, E. T. (2017). Inferring Carbon Abatement Costs in Electricity Markets: A Revealed Preference Approach using the Shale Revolution. *American Economic Journal: Economic Policy*, 9(3):106–33.

Currie, J. and Neidell, M. (2005). Air Pollution and Infant Health: What Can We Learn From California's Recent Experience?*. *Quarterly Journal of Economics*, 120(3):1003–1030.

Currie, J., Neidell, M., and Schmieder, J. F. (2009). Air pollution and infant health: Lessons from new jersey. *Journal of health economics*, 28(3):688–703.

Currie, J. and Walker, R. (2011). Traffic congestion and infant health: Evidence from e-zpass. *American Economic Journal: Applied Economics*, 3(1):65–90.

Currie, J., Zivin, J. G., Mullins, J., and Neidell, M. (2014). What do we know about short-and long-term effects of early-life exposure to pollution? *Annu. Rev. Resour. Econ.*, 6(1):217–247.

Edenhofer, O., Hirth, L., Knopf, B., Pahle, M., Schlömer, S., Schmid, E., and Ueckerdt, F. (2013). On the economics of renewable energy sources. *Energy Economics*, 40:S12–S23.

Fell, H. and Kaffine, D. T. (2018). The Fall of Coal: Joint Impacts of Fuel Prices and Renewables on Generation and Emissions. *American Economic Journal: Economic Policy*, 10(2):90–116.

Fell, H., Kaffine, D. T., and Novan, K. (2019). Emissions, transmission, and the environmental value of renewable energy. Technical report.

Fell, H. and Linn, J. (2013). Renewable Electricity Policies, Heterogeneity, and Cost Effectiveness. *Journal of Environmental Economics and Management*, 66(3):688–707.

Franklin, B. A., Brook, R., and Pope III, C. A. (2015). Air pollution and cardiovascular disease. *Current problems in cardiology*, 40(5):207–238.

Galetovic, A. and Muñoz, C. M. (2011). Regulated Electricity Retailing in Chile. *Energy policy*, 39(10):6453–6465.

Gauderman, W. J., Avol, E., Lurmann, F., Kuenzli, N., Gilliland, F., Peters, J., and McConnell, R. (2005). Childhood Asthma and Exposure to Traffic and Nitrogen Dioxide. *Epidemiology*, 16(6):737–743.

Guallar, E., Sanz-Gallardo, M. I., Veer, P. v., Bode, P., Aro, A., Gómez-Aracena, J., Kark, J. D., Riemersma, R. A., Martín-Moreno, J. M., and Kok, F. J. (2002). Mercury, fish oils, and the risk of myocardial infarction. *New England Journal of Medicine*, 347(22):1747–1754.

Guidetti, B., Pereda, P., and Severnini, E. (2020). Health shocks under hospital capacity constraint: Evidence from air pollution in sao paulo, brazil.

Gupta, A. and Spears, D. (2017). Health externalities of india's expansion of coal plants:

Evidence from a national panel of 40,000 households. *Journal of environmental economics and management*, 86:262–276.

Haas, J., Palma-Behnke, R., Valencia, F., Araya, P., Díaz-Ferrán, G., Telsnig, T., Eltrop, L., Díaz, M., Püschel, S., Grandel, M., et al. (2018). Sunset or sunrise? understanding the barriers and options for the massive deployment of solar technologies in chile. *Energy Policy*, 112:399–414.

Hoek, G., Krishnan, R. M., Beelen, R., Peters, A., Ostro, B., Brunekreef, B., and Kaufman, J. D. (2013). Long-term air pollution exposure and cardio-respiratory mortality: a review. *Environmental health*, 12(1):43.

Holladay, J. S. and LaRiviere, J. (2017). The Impact of Cheap Natural Gas on Marginal Emissions from Electricity Generation and Implications for Energy Policy. *Journal of Environmental Economics and Management*, 85:205–227.

Jacques-Coper, M., Falvey, M., and Muñoz, R. C. (2015). Inter-daily variability of a strong thermally-driven wind system over the atacama desert of south america: synoptic forcing and short-term predictability using the gfs global model. *Theoretical and Applied Climatology*, 121(1-2):211–223.

Kaffine, D. T., McBee, B. J., and Lieskovsky, J. (2013). Emissions Savings from Wind Power Generation in Texas. *The Energy Journal*, 34(1).

Kline, P. and Walters, C. R. (2016). Evaluating public programs with close substitutes: The case of head start. *The Quarterly Journal of Economics*, 131(4):1795–1848.

Knittel, C. R., Metaxoglou, K., and Trindade, A. (2015). Natural Gas Prices and Coal Displacement: Evidence from Electricity Markets. Technical report, National Bureau of Economic Research.

Knittel, C. R., Miller, D. L., and Sanders, N. J. (2016). Caution, Drivers! Children Present: Traffic, Pollution, and Infant Health. *Review of Economics and Statistics*, 98(2):350–366.

Kopas, J., York, E., Jin, X., Harish, S., Kennedy, R., Shen, S. V., and Urpelainen, J. (2020). Environmental justice in india: Incidence of air pollution from coal-fired power plants. *Ecological Economics*, 176:106711.

Linn, J., Mastrangelo, E., and Burtraw, D. (2014). Regulating Greenhouse Gases from Coal Power Plants under the Clean Air Act. *Journal of the Association of Environmental and Resource Economists*, 1(1/2):97–134.

Linn, J. and Muehlenbachs, L. (2018). The Heterogeneous Impacts of Low Natural Gas

Prices on Consumers and the Environment. *Journal of Environmental Economics and Management*, 89:1–28.

Lu, X., Salovaara, J., and McElroy, M. B. (2012). Implications of the Recent Reductions in Natural Gas Prices for Emissions of CO_2 from the US Power Sector. *Environmental science & technology*, 46(5):3014–3021.

Millstein, D., Wiser, R., Bolinger, M., and Barbose, G. (2017). The Climate and Air-Quality Benefits of Wind and Solar Power in the United States. *Nature Energy*, 2(9):17134.

Ministry of Energy (2013). Ley 20.698: Propicia la ampliación de la matriz energética mediante fuentes renovables no convencionales. Retrieved from Congreso Nacional de Chile.

Muller, N. Z. and Mendelsohn, R. (2009). Efficient pollution regulation: getting the prices right. *American Economic Review*, 99(5):1714–39.

Muñoz, R. C., Falvey, M. J., Arancibia, M., Astudillo, V. I., Elgueta, J., Ibarra, M., Santana, C., and Vásquez, C. (2018). Wind energy exploration over the atacama desert: A numerical model–guided observational program. *Bulletin of the American Meteorological Society*, 99(10):2079–2092.

Neidell, M. (2009). Information, avoidance behavior, and health the effect of ozone on asthma hospitalizations. *Journal of Human resources*, 44(2):450–478.

Novan, K. (2015). Valuing the Wind: Renewable Energy Policies and Air Pollution Avoided. *American Economic Journal: Economic Policy*, 7(3):291–326.

Orehek, J., Massari, J. P., Gayrard, P., Grimaud, C., and Charpin, J. (1976). Effect of short-term, low-level nitrogen dioxide exposure on bronchial sensitivity of asthmatic patients. *Journal of Clinical Investigation*, 57(2):301–307.

Pershagen, G., Rylander, E., Norberg, S., Eriksson, M., and Nordvall, S. L. (1995). Air Pollution Involving Nitrogen Dioxide Exposure and Wheezing Bronchitis in Children. *International Journal of Epidemiology*, 24(6):1147–1153.

Programa Chile Sustentable (2017). Termoelétricas a Carbón en Chile. http://www.chilesustentable.net. Retrieved in March, 2020.

Rivera, N. M. (2020). Is mining an environmental disamenity? evidence from resource extraction site openings. *Environmental and Resource Economics*, 75(3):485–528.

Rondanelli, R., Molina, A., and Falvey, M. (2015). The Atacama surface Solar Maximum. *Bulletin of the American Meteorological Society*, 96(3):405–418.

Ruiz-Rudolph, P., Arias, N., Pardo, S., Meyer, M., Mesías, S., Galleguillos, C., Schiattino, I., and Gutiérrez, L. (2016). Impact of Large Industrial Emission Sources on Mortality and Morbidity in Chile: A Small-Areas Study. *Environment international*, 92:130–138.

Salonen, J. T., Seppänen, K., Nyyssönen, K., Korpela, H., Kauhanen, J., Kantola, M., Tuomilehto, J., Esterbauer, H., Tatzber, F., and Salonen, R. (1995). Intake of mercury from fish, lipid peroxidation, and the risk of myocardial infarction and coronary, cardiovascular, and any death in eastern finnish men. *Circulation*, 91(3):645–655.

Schlenker, W. and Walker, W. R. (2016). Airports, air pollution, and contemporaneous health. *The Review of Economic Studies*, 83(2):768–809.

Schwartz, J. (1996). Air pollution and hospital admissions for respiratory disease. *Epidemiology*, pages 20–28.

Schwartz, J. and Morris, R. (1995). Air pollution and hospital admissions for cardiovascular disease in detroit, michigan. *American journal of epidemiology*, 142(1):23–35.

Sergi, B., Adams, P. J., Muller, N., Robinson, A. L., Davis, S., Marshall, J. D., and Azevedo, I. M. L. (2020). Optimizing emissions reductions from the us power sector for climate and health benefits. *Environmental Science & Technology*.

Siler-Evans, K., Azevedo, I. L., Morgan, M. G., and Apt, J. (2013). Regional Variations in the Health, Environmental, and Climate Benefits of Wind and Solar Generation. *Proceedings of the National Academy of Sciences*, 110(29):11768–11773.

Spiller, E., Sopher, P., Martin, N., Mirzatuny, M., and Zhang, X. (2017). The environmental impacts of green technologies in tx. *Energy Economics*, 68:199–214.

Stocker, T. F., Qin, D., Plattner, G.-K., Tignor, M., Allen, S. K., Boschung, J., Nauels, A., Xia, Y., Bex, V., Midgley, P. M., et al. (2013). Climate change 2013: The physical science basis. *Contribution of working group I to the fifth assessment report of the intergovernmental panel on climate change*, 1535.

Thakrar, S. K., Balasubramanian, S., Adams, P. J., Azevedo, I. M., Muller, N. Z., Pandis, S. N., Polasky, S., Pope III, C. A., Robinson, A. L., Apte, J. S., et al. (2020). Reducing mortality from air pollution in the united states by targeting specific emission sources. *Environmental Science & Technology Letters*, 7(9):639–645.

Trasande, L., Landrigan, P. J., and Schechter, C. (2005). Public health and economic

consequences of methyl mercury toxicity to the developing brain. *Environmental health perspectives*, 113(5):590–596.

U.S. Energy Information Administration (2019). International Energy Outlook 2019. Retrieved in November, 2019.

U.S. Environmental Protection Agency (2006). Air Quality Criteria Document for Ozone. https://cfpub.epa.gov/ncea/risk/recordisplay.cfm?deid=149923. Retrieved in December, 2020.

U.S. Environmental Protection Agency (2014). EPA's Report on the Environment (ROE): Sulfur Dioxide Emissions. https://cfpub.epa.gov/roe/indicator.cfm?i=22. Last Updated: 2014.

U.S. Environmental Protection Agency (2015). EPA's Report on the Environment (ROE): Mercury Emissions. https://cfpub.epa.gov/roe/indicator.cfm?i=14. Last Updated: 2015.

U.S. Environmental Protection Agency (2019). Local Renewable Energy Benefits and Resources. https://www.epa.gov/statelocalenergy/local-renewable-energy-benefits-and-resources. Retrieved in November, 2019.

Wiser, R., Mai, T., Millstein, D., Barbose, G., Bird, L., Heeter, J., Keyser, D., Krishnan, V., and Macknick, J. (2017). Assessing the costs and benefits of us renewable portfolio standards. *Environmental Research Letters*, 12(9):094023.

Wooldridge, J. M. (2010). *Econometric analysis of cross section and panel data*. MIT press.

Wooldridge, J. M. (2015). Control function methods in applied econometrics. *Journal of Human Resources*, 50(2):420–445.

World Health Organization (2006). *Air Quality Guidelines*. Global Update 2005. World Health Organization.

Appendix

Table A1: Descriptive Statistics - Other Covariates

Variable	Mean	Std. Dev.	Min.	Max.
Panel A. All cities (= 19)				
Demographics:				
Population	61,802.89	104,603.38	244	395,453
Density	19.43	47.45	0.08	229.51
Poverty Rate	14.11	9.06	2	37
Fertility Rate	11.18	6.32	0	21.6
Weather:				
Min. Temp. (C)	7.10	6.34	-25	23
Max. Temp. (C)	10.72	8.65	-11.8	33.4
Humidity (%)	49.11	13.71	9.68	96.26
Panel B. Cities with fossil fuel generation (= 5)				
Demographics:				
Population	167,575	140,344.43	11,090	395,453
Density	30.91	32.35	2.92	89.28
Poverty Rate	8.30	3.66	3.12	15.71
Fertility Rate	16.31	2.13	12.19	21.6
Weather:				
Min. Temp. (C)	9.03	6.67	-18.4	23
Max. Temp. (C)	13.46	8.72	-11.8	33.4
Humidity (%)	52.31	14.07	9.69	96.26
Panel C. Cities without fossil fuel generation (= 13)				
Demographics:				
Population	25,041.19	51,812.2	244	184,543
Density	16.42	53.11	0.08	229.51
Poverty Rate	16.29	9.82	2	37
Fertility Rate	9.40	6.49	0	20.99
Weather:				
Min. Temp. (C)	6.40	6.09	-25	22
Max. Temp. (C)	9.98	8.52	-11.8	33
Humidity (%)	47.88	13.68	9.68	95.85

Notes: Data from SINIM. Observations are at the city level. There is one city in our sample, Pica, that switches from panel C to panel B due to the opening of a new fossil fuel generator. We discard this city from panels B and C.

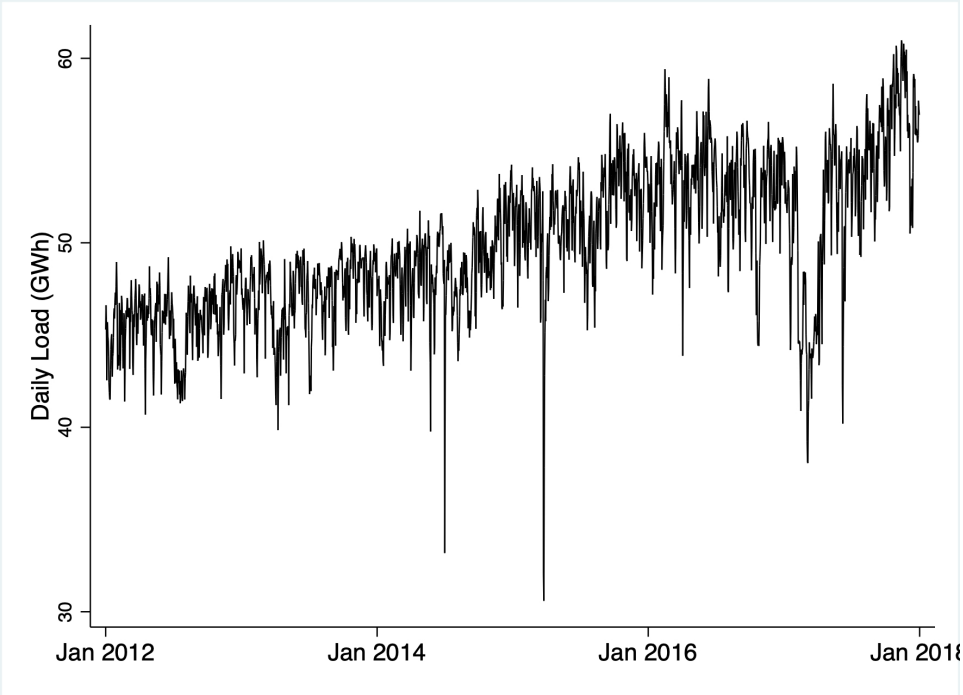

Figure A1: SING's Daily Load

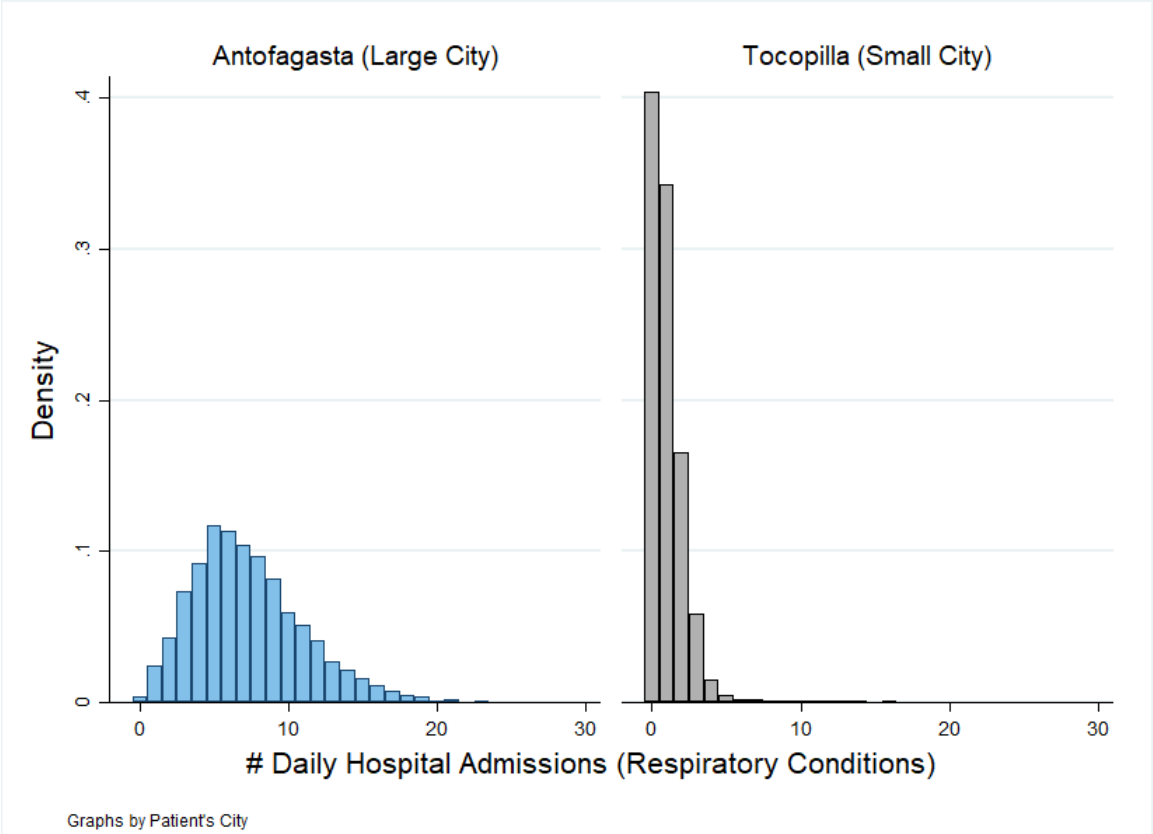

Figure A2: Overdispersion in the Health Outcome Variables

Notes: The left-hand panel exhibits the number of daily hospital admissions due to respiratory conditions for one of the largest cities in the sample, Antofagasta, while the right-hand panel shows the same variable for the case of a smaller city, Tocopilla. The overdispersion of this variable is evident in the case of the large city (left-hand side). The heterogeneity in the size of the pile-up at zero is also clear when comparing the two cities.

Table A2: The Effect of Solar on Daily Aggregated Fossil Fuels Generation (Single-Fuel Engines)

	Coal		Diesel		Fuel oil		Fuel oil #6	
	(1)	(2)	(1)	(2)	(1)	(2)	(1)	(2)
Generation (GWh)	-0.813***	-0.813***	-0.017	-0.017	-0.011	-0.011	0.001	0.001
	(0.137)	(0.137)	(0.011)	(0.011)	(0.023)	(0.023)	(0.001)	(0.001)
Capacity factor	-0.022***	-0.022***	-0.009**	-0.009**	0.047	0.047	0.029	0.029
	(0.004)	(0.004)	(0.004)	(0.004)	(0.047)	(0.047)	(0.018)	(0.018)
Obs.	1,915	1,915	1,915	1,915	910	910	1,825	1,825
Controls	×	×	×	×	×	×	×	×
τ_1 fixed effects	×		×		×		×	
τ_2 fixed effects		×		×		×		×

Notes: Marginal effects of 1 GWh of daily solar generation are derived from an OLS on daily aggregated generation, and from a fractional logit response model on daily capacity factors. Estimations include plants reporting a single fuel use. Controls include daily temperature, humidity, load and price ratios. Vector τ_1 includes year, month, and weekend fixed effects. Vector τ_2 includes year, seasons, year × seasons, and weekend fixed effects. Bootstrapped standard errors appear in parentheses. Significance levels: $^{*}p < 0.10$, $^{**}p < 0.05$, $^{***}p < 0.001$.

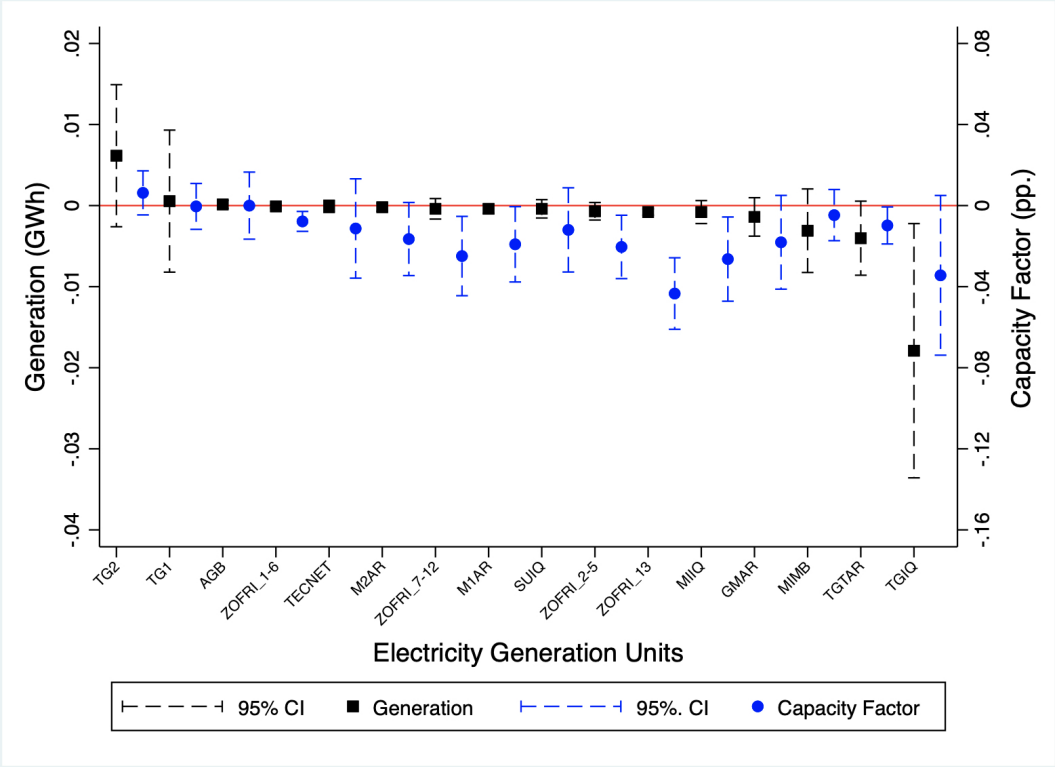

Figure A3: Diesel-Fired (Single-Fuel) EGUs and Displacement

Notes: We use all single-fuel EGUs that report diesel as their primary fuel source. We exclude units with dual engines that run with natural gas or that report using fuel oil as well. The left y-axis shows the marginal effects of 1 GWh of daily solar generation on plant-level daily generation using OLS. The right y-axis shows the marginal effects of 1 GWh of daily solar generation on daily capacity factors using a fractional logit response model. The estimation equation is identical to the one in columns (2) of 4. Dashed lines represent 95% confidence intervals obtained with bootstrapped standard errors.

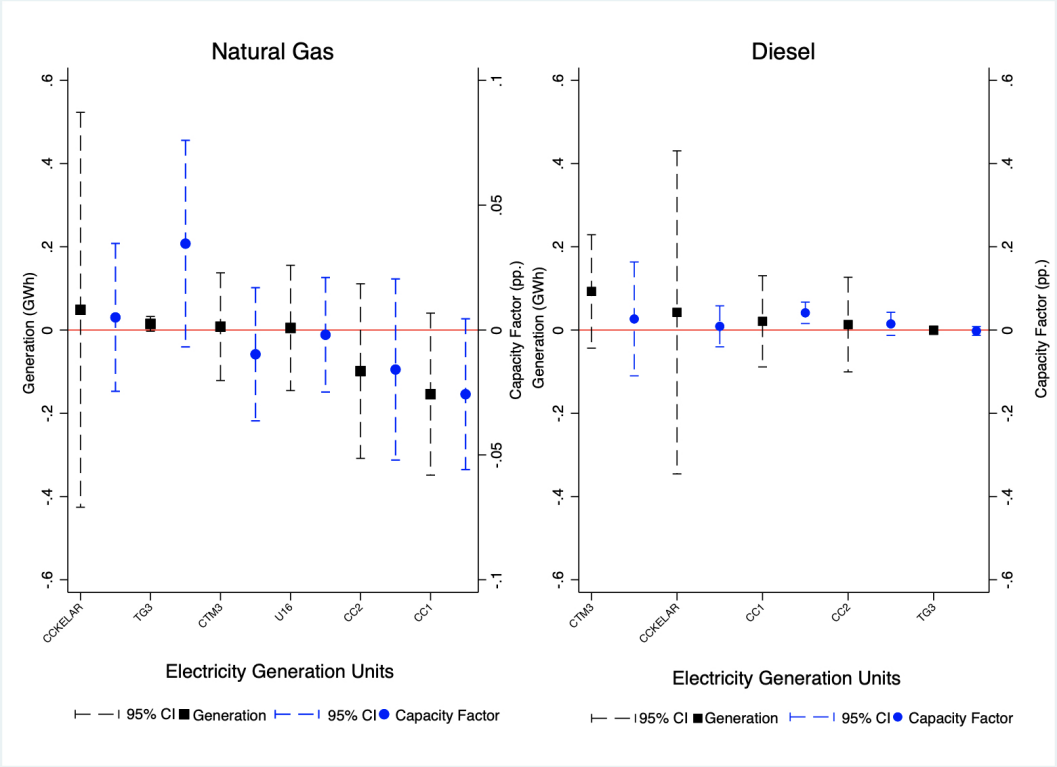

Figure A4: Natural Gas-Fired (Combined-Cycle) EGUs and Displacement

Notes: We use all CC EGUs that report natural gas as their primary fuel source. The left-hand panel shows natural gas use, while the right-hand panel shows diesel use. The left y-axis shows the marginal effects of 1 GWh of daily solar generation on plant-level daily generation using OLS. The right y-axis shows the marginal effects of 1 GWh of daily solar generation on daily capacity factors using a fractional logit response model. The estimation equation is identical to the one in columns (2) of Table 4. Dashed lines represent 95% confidence intervals obtained with bootstrapped standard errors.

Table A3: The Effect of 1 GWh of Solar Generation on Hospital Admissions by Age Group for Cities $< 50km$ and $< 100km$ Downwind of Displaced Fossil Fuel Plants

	Cities $< 50km$ Downwind of Displaced Fossil Fuel Plants					Cities $< 100km$ Downwind of Displaced Fossil Fuel Plants				
	Infants	Toddlers	Children	Adults	Seniors	Infants	Toddlers	Children	Adults	Seniors
Panel A. Cardiovascular										
Solar_d	-0.0002	-0.0004	-0.0004	-0.018	-0.012	-0.0002	-0.0005	-0.0002	-0.019	-0.009
	(0.038)	(0.008)	(0.003)	(0.026)	(0.019)	(0.005)	(0.003)	(0.002)	(0.018)	(0.017)
Panel B. All respiratory										
Solar_d	-0.039*	-0.025	-0.012	-0.002	-0.011	-0.031***	-0.022**	-0.008	-0.004	-0.009**
	(0.022)	(0.032)	(0.054)	(0.010)	(0.040)	(0.009)	(0.010)	(0.009)	(0.013)	(0.004)
Panel C. Upper respiratory										
Solar_d	0.0003	-0.006	-0.016	0.002	-0.0008	0.0003	-0.003	-0.012**	-0.001	-0.001
	(0.003)	(0.008)	(0.015)	(0.011)	(0.006)	(0.002)	(0.003)	(0.004)	(0.014)	(0.003)
Panel D. Lower respiratory										
Solar_d	-0.038	-0.017	-0.002	-0.008	-0.012	-0.030***	-0.018	-0.001	-0.008	-0.011
	(0.041)	(0.014)	(0.044)	(0.019)	(0.085)	(0.007)	(0.012)	(0.013)	(0.013)	(0.043)
Obs.	5,745	5,745	5,745	5,745	5,745	7,660	7,660	7,660	7,660	7,660
Controls	×	×	×	×	×	×	×	×	×	×
City Fixed Effects	×	×	×	×	×	×	×	×	×	×
τ_2	×	×	×	×	×	×	×	×	×	×

Notes: Marginal effects from ZINB panel-data regressions using 100 iterations. Inflate regressions at count zero are estimated using a logit estimator. Controls include weather, mining production and demographic covariates (including population) in both the main and the inflate regressions. Vector τ_2 includes year, seasons, year × seasons, and weekend fixed effects. Clustered standard errors by city appear in parentheses. Significance levels: $^{*}p < 0.10$, $^{**}p < 0.05$, $^{***}p < 0.001$.

Table A4: The Long-Term Effect of 1 GWh of Solar Generation on Daily Hospital Admissions

	All Cities			Cities Downwind of Displaced Fossil Fuel Plants								
				$< 10km$			$< 50km$			$< 100km$		
	t=week	t=month	t=year	t=week	t=month	t=year	t=week	t=month	t=year	t=week	t=month	t=year
INFANTS												
Panel A. Cardiovascular												
Solar_t	-0.0001	-0.0001	-0.0001	-0.0001	-0.0003	-0.001	-0.0002	-0.0002	-0.001	-0.0001	-0.0001	-0.0005
	(0.006)	(0.0003)	(0.007)	(0.002)	(0.005)	(0.006)	(0.001)	(0.004)	(0.010)	(0.002)	(0.001)	(0.009)
Panel B. All respiratory												
Solar_t	-0.026**	-0.016	0.050	-0.050	-0.054*	-0.013	-0.053**	-0.043	-0.010	-0.041*	-0.030	-0.008
	(0.013)	(0.041)	(0.071)	(0.034)	(0.032)	(0.102)	(0.020)	(0.028)	(0.330)	(0.024)	(0.090)	(0.042)
Panel C. Upper respiratory												
Solar_t	0.001	-0.0002	0.00002	-0.001	-0.001	0.001	-0.001	-0.0001	0.0005	-0.0004	0.000002	0.0005
	(0.0004)	(0.002)	(0.013)	(0.007)	(0.004)	(0.004)	(0.006)	(0.002)	(0.008)	(0.005)	(0.001)	(0.003)
Panel D. Lower respiratory												
Solar_t	-0.014	-0.010	-0.004	-0.041	-0.049	-0.008	-0.048	-0.038	-0.010	-0.036**	-0.031	-0.007
	(0.013)	(0.018)	(0.100)	(0.180)	(0.030)	(0.080)	(0.033)	(0.032)	(0.046)	(0.015)	(0.030)	(0.336)
TODDLERS												
Panel A. Cardiovascular												
Solar_t	-0.001	-0.001	-0.001	-0.002	-0.001	-0.002	-0.002	-0.001	-0.002	-0.001	-0.001	-0.001
	(0.001)	(0.005)	(0.142)	(0.004)	(0.019)	(0.005)	(0.054)	(0.004)	(0.003)	(0.009)	(0.007)	(0.004)
Panel B. All respiratory												
Solar_t	-0.008	-0.006	-0.006	-0.027	-0.001	0.030	-0.024	-0.009	0.005	-0.022	-0.011*	0.003
	(0.008)	(0.009)	(0.017)	(0.044)	(0.065)	(0.070)	(0.081)	(0.021)	(0.141)	(0.028)	(0.007)	(0.010)
Panel C. Upper respiratory												
Solar_t	-0.004	-0.008	-0.015*	-0.013	-0.007	-0.007	-0.006	-0.002	0.003	-0.003	-0.001	0.001
	(0.006)	(0.006)	(0.009)	(0.012)	(0.084)	(0.162)	(0.012)	(0.018)	(0.013)	(0.025)	(0.193)	(0.056)
Panel D. Lower respiratory												
Solar_t	-0.005	-0.002	0.0004	-0.013	-0.008	0.009	-0.018	-0.006	0.004	-0.017	-0.009*	0.002
	(0.004)	(0.004)	(0.015)	(0.042)	(0.050)	(0.121)	(0.016)	(0.435)	(0.078)	(0.020)	(0.005)	(0.016)
CHILDREN												
Panel A. Cardiovascular												
Solar_t	-0.001	-0.001	-0.002	-0.0004	-0.0001	-0.001	0.0001	0.0003	-0.0002	-0.00002	0.0001	-0.0003
	(0.003)	(0.003)	(0.064)	(0.009)	(0.011)	(0.019)	(0.003)	(0.020)	(0.022)	(0.028)	(0.013)	(0.015)
Panel B. All respiratory												
Solar_t	-0.005	-0.004	-0.006	-0.006	0.002	0.008	-0.018	0.007	0.030	-0.008	0.004	0.017
	(0.010)	(0.008)	(0.012)	(0.047)	(0.105)	(0.366)	(0.158)	(0.055)	(0.031)	(0.090)	(0.020)	(0.081)
Panel C. Upper respiratory												
Solar_t	-0.013	-0.010*	-0.013	-0.010	-0.007	-0.0004	-0.024**	-0.012	-0.004	-0.012**	-0.008	0.012
	(0.030)	(0.006)	(0.013)	(0.018)	(0.012)	(0.069)	(0.011)	(0.010)	(0.023)	(0.005)	(0.008)	(0.029)
Panel D. Lower respiratory												
Solar_t	0.003	0.002	0.002	0.002	0.0005	0.013	0.002	0.007	0.010	0.003	0.005	0.008
	(2.181)	(0.003)	(0.005)	(0.008)	(0.606)	(0.209)	(0.003)	(0.006)	(0.036)	(0.004)	(0.006)	(0.016)
Obs.	36,366	36,366	36,366	3,828	3,828	3,828	5,742	5,742	5,742	7,656	7,656	7,656
Controls	×	×	×	×	×	×	×	×	×	×	×	×
City fixed effects	×	×	×	×	×	×	×	×	×	×	×	×
τ_2 fixed effects	×	×	×	×	×	×	×	×	×	×	×	×

Notes: Marginal effects from ZINB panel-data regressions using 100 iterations. Inflate regressions at count zero are estimated using a logit estimator. Controls include weather, mining production and demographic covariates (including population) in both the main and the inflate regressions. Vector τ_2 includes year, seasons, year × seasons, and weekend fixed effects. Clustered standard errors by city appear in parentheses. Significance levels: $^{*}p < 0.10$, $^{**}p < 0.05$, $^{***}p < 0.001$.

Table A5: The Long-Term Effect of 1 GWh of Solar Generation on Daily Hospital Admissions (Cont.)

	All Cities			Cities Downwind of Displaced Fossil Fuel Plants								
				$< 10km$			$< 50km$			$< 100km$		
	t=week	t=month	t=year	t=week	t=month	t=year	t=week	t=month	t=year	t=week	t=month	t=year
ADULTS												
Panel A. Cardiovascular												
Solar_t	-0.015	-0.016	-0.033*	-0.035	-0.040	-0.062	-0.028	-0.040	-0.051	-0.030	-0.033**	-0.068***
	(0.011)	(0.012)	(0.019)	(1.048)	(0.092)	(0.143)	(0.062)	(0.166)	(0.036)	(0.021)	(0.015)	(0.012)
Panel B. All respiratory												
Solar_t	-0.005	-0.005	-0.006	-0.010	0.007	0.029	0.002	0.016	0.028	-0.002	0.010	0.021**
	(0.087)	(0.050)	(0.019)	(0.018)	(0.037)	(0.030)	(0.108)	(0.022)	(0.074)	(0.032)	(0.010)	(0.009)
Panel C. Upper respiratory												
Solar_t	-0.005	-0.006	-0.011	-0.002	-0.0003	0.002	0.004	-0.029***	0.010	-0.0005	0.001	0.001
	(0.005)	(0.004)	(0.008)	(0.206)	(10.33)	(0.772)	(0.009)	(0.006)	(0.012)	(0.059)	(0.030)	(0.018)
Panel D. Lower respiratory												
Solar_t	0.001	0.001	0.005	0.002	0.008	0.020	-0.007	0.005	0.016	-0.007	0.001	0.011
	(0.005)	(0.005)	(0.012)	(0.061)	(0.301)	(4.227)	(0.021)	(0.021)	(0.030)	(0.026)	(0.015)	(0.017)
SENIORS												
Panel A. Cardiovascular												
Solar_t	-0.006	-0.016	-0.007	-0.021	-0.024	-0.035	-0.013	-0.017	-0.037	-0.012	-0.014	-0.027
	(0.014)	(0.017)	(0.042)	(0.042)	(0.058)	(0.106)	(0.026)	(0.035)	(0.068)	(0.015)	(0.051)	(0.220)
Panel B. All respiratory												
Solar_t	-0.013*	-0.011	0.001	-0.022	-0.020	-0.014	-0.021	-0.017	-0.010	-0.015	-0.013	-0.002
	(0.007)	(0.008)	(0.026)	(0.071)	(0.014)	(0.035)	(0.052)	(0.079)	(0.045)	(0.010)	(0.043)	(0.045)
Panel C. Upper respiratory												
Solar_t	-0.001	-0.001	-0.001	-0.001	-0.001***	-0.002	-0.001	-0.001*	-0.002	-0.001	-0.001	-0.001
	(0.001)	(0.013)	(0.023)	(0.001)	(0.0001)	(0.011)	(0.003)	(0.0004)	(0.003)	(0.001)	(0.009)	(0.015)
Panel D. Lower respiratory												
Solar_t	-0.002	-0.0001	0.005	-0.025***	-0.018	-0.004	-0.021	-0.017	-0.004	-0.018	-0.012	-0.0002
	(0.007)	(0.009)	(0.046)	(0.007)	(0.024)	(0.049)	(0.015)	(0.018)	(0.026)	(0.014)	(0.10)	(0.024)
Obs.	36,366	36,366	36,366	3,828	3,828	3,828	5,742	5,742	5,742	7,656	7,656	7,656
Controls	×	×	×	×	×	×	×	×	×	×	×	×
City fixed effects	×	×	×	×	×	×	×	×	×	×	×	×
τ_2 fixed effects	×	×	×	×	×	×	×	×	×	×	×	×

Notes: Marginal effects from ZINB panel-data regressions using 100 iterations. Inflate regressions at count zero are estimated using a logit estimator. Controls include weather, mining production and demographic covariates (including population) in both the main and the inflate regressions. Vector τ_2 includes year, seasons, year × seasons, and weekend fixed effects. Clustered standard errors by city in parentheses. Significance levels: $^{*}p < 0.10$, $^{**}p < 0.05$, $^{***}p < 0.001$.